

# Modeling and Optimization of an Industrial Ammonia Synthesis Unit: An Exergy Approach

*Daniel Flórez-Orrego<sup>a</sup>, Silvio de Oliveira Junior<sup>b</sup>*

*Department of Mechanical Engineering, Polytechnic School, University of Sao Paulo, Sao Paulo, 05508-900, Brazil. <sup>a</sup>daflorez@usp.br CA, <sup>b</sup>soj@usp.br*

## Abstract:

An exergy modeling and optimization of an industrial ammonia unit based on steam methane reforming (SMR) process is presented. The base-case unit produces about 1000 t NH<sub>3</sub>/day [1], as well as power and steam, with no auxiliary exergy use. Some critical operation parameters are analyzed and the base-case and optimal operating conditions of the major components are compared. Since the ammonia synthesis process is highly exothermic, higher per-pass conversions in industrial adiabatic reactors are often achieved by using various sequential catalyst beds, where a near-optimum profile of reaction rate vs temperature can be attained by regulating the inlet temperature of each bed. This is performed via internal heat recovery, either by preheating reactor feed gas or by using waste heat boilers, which results in an increase of the steam production and a smaller fuel consumption. But, although such near-optimum operation conditions may lead to higher reaction rates and, thus, lower catalyst volumes could be required, it is found that the optimal design of the ammonia loop is rather determined by the performance of each component and their interdependencies. Moreover, since the proposed objective function (exergy destruction minimization) is very sensitive to specific process variables, the convergence of the solution algorithm is sometimes hindered. The exergy destruction breakdown shows that the ammonia converter and the refrigeration system are together responsible for more than 71-82% of the total exergy destruction in the ammonia loop, which in turn varies between 25.6 - 38.8 MW for optimal and base-case operation conditions, respectively.

## Keywords:

Ammonia, Optimization, Exergy Destruction, Exothermic Reactions, Counteraction Principle

## 1. Introduction

More than 60% of the Brazilian nitrogen fertilizer consumption must still be imported [2] despite the growing volumes of domestic production [3, 4], which leaves the country vulnerable to variations in prices in the international markets, natural gas prices, shipping costs and logistical problems at its ports [5]. In fact, fertilizers industry is the segment that has contributed the most (25%) towards the total deficit in the Brazilian chemical sector [6], and its technological and economic lags are partially owed to lower efficiencies of existing plants. Aiming to reduce the foreign dependence of the Brazilian fertilizers sector to only 13% in 2020 [7], as well as to meet more stringent controls of plant emissions, further investments in the construction of new plants or revamping the old ones are contemplated [2, 6-8]. However, new facilities require high initial capital investments, while retrofitting old plants poses a challenge because of the increased flows. Besides, these facilities have a complex design in which multiple processes should be coupled and integrated in terms of mass and energy flows via recycled streams. Thus, the overall system is not only large in magnitude, but the multiple interdependencies lead to a complex non-linear problem. Accordingly, a systematic framework to compare the benefits of revamping or substituting the outdated technologies is required.

Papoulias and Grossman [9] presented an strategy based on mixed-integer programming for the optimal synthesis of a chemical plant, including the ammonia loop, with a heat recovery network and an utility system. Notwithstanding the strategy accounts explicitly for the interactions among the three components, the influence of the process kinetics, equilibrium conversion, layout and intercooling system of catalytic beds and other loop parameters on the performance of the whole ammonia unit, were not considered. By considering the thermodynamic minimum energy

consumption using steam methane reforming route, Worrell and Blok [10] calculated the effect that the energy savings in ammonia production may have on the manufacturing of several nitrogen fertilizers. The authors suggested that profitable energy savings would be only obtained by means of technical breakthroughs such as single synthesis loops with higher conversions at lower pressures and more efficient heat transfer processes. Anyhow, depending on the investment criteria and payback period, savings of only 6% are achievable from a total technical potential of 16%.

Leites *et al* [11] studied the causes of thermodynamic irreversibility in chemical reactions and other industrial chemical processes in ammonia plants based on the counteraction principle. It is shown that conflicting objectives may arise from the minimization of the process irreversibilities while simultaneously aiming to increase the driving forces, with special attention to reactive separation and exothermic reactors. According to Kirova-Yordanova [12], the exergy consumption in the ammonia synthesis loop is highly dependent on the designed configuration, and at least 61% of destroyed exergy comes from ammonia converter. It is concluded that the only way to reduce consumption and, thus, to improve the overall exergy efficiency of ammonia plants is the utilization of the reaction enthalpy at a higher level of temperature for HP steam generation. Panjeshahi *et al.* [13] studied the retrofitting opportunities of an existing ammonia plant based on suitable modifications of the current heat exchanger network, especially in the reformer convection train, which was separately considered as a hot threshold problem. The so-called cold threshold problem, basically composed of the back-end ammonia production loop, was analyzed by using the Carnot grand composite curve profile (combined pinch and exergy method) in order to determine the extent of the integration of the refrigeration cycle already in use, and suggest the most appropriate temperature levels that allowed reducing the system irreversibilities and shaft power consumption. However, conflicting results arose while retrofitting the refrigeration temperatures, since the heat exchange driving forces are also reduced, requiring larger heat exchanger areas or heat transfer coefficients. Tock and Maréchal [14] studied the ammonia production by using natural gas and biomass. A consistent thermo-environmental optimization approach is applied for the conceptual process design and competitiveness evaluation. By considering the biogenic nature of the carbon in the biomass, the emissions are reported to drop to  $-1.79 \text{ kg}_{\text{CO}_2}/\text{kg}_{\text{NH}_3}$  for the biomass process, which has an energy efficiency of 50%. In projected large capacity ammonia plants [15], the main problems have been reported for the increased compressor capacity, higher operating pressures and the need of nitrogen washing, not to mention the bottlenecking capacity of the reformer duty.

Even if after years of intensive research the margins for a substantial drop of the specific exergy consumption have become small, the minimum theoretical exergy consumption in ammonia plants is still somewhat lower ( $18\text{-}21 \text{ GJ}/\text{t}_{\text{NH}_3}$ ) [16] than the best figures reported in the literature ( $28\text{-}31 \text{ GJ}/\text{t}_{\text{NH}_3}$ ), which vary widely with local conditions and project-specific requirements [17, 18]. According to The European Roadmap of Process Intensification (PI - PETCHEM), there are still potential benefits in the ammonia production sector. They amount to a 5% higher overall energy efficiency for the short/midterm (10-20 years) and 20% higher (30-40 years) for the long term [19]. Other studies [20] are less optimistic and estimate that the improvement factor must continue at a lower rate than experienced over 1991-2003, i.e. the fuel consumption improvement must be 35% less than during the previous decade. Despite this scenario, they also admit the potentials benefits of further process integration during the design of new ammonia and urea plants, with lower or minor incremental capital costs and with a reduced carbon emission-to-ammonia throughput ratio. Some non-conventional attempts for improving the energy and mass integration which have not been industrially explored so far due to technical or economical aspects include more active catalyst sources at lower temperatures [21], monolith reactors [22], low-grade temperature heat valorization, thermally coupled reactions [23] or in situ adsorption reactors [24], as well the substitution of the reactor effluent recovery heat exchanger by expanders so that the thermal exergy available is more rationally recovered [25, 26]. Even if they could take too much time to reach a commercial introduction or to be practically accomplished, they show a further insight into the thermodynamic limitations with which the reduction of energy consumption in ammonia production copes with.

On the other hand, exergy saving steps without an alternative use for saved exergy does not represent an economic criteria for making large capital investments, since some modifications are not always economical and even may adversely affect reliability [27]. Accordingly, caution is suggested when comparing the potential exergy savings against potential economic and environmental gains. Anyhow, increasing the efficiency of the domestic production share can be the first step towards the reduction of the large non-renewable exergy consumption and environmental impact that ammonia is responsible for. Thus, in this work, exergy is used to quantify the efficiency and minimize the exergy destruction rate along the various components of the ammonia synthesis loop as well as to optimize its revenues as a function of the most critical operation parameters. It will be shown that the optimal design is rather a complex function of the standalone equipment performance and the interaction of all the synthesis loop components, even though largely influenced by the reactor performance.

## 2. Synthesis unit description

The ammonia synthesis unit includes the fresh syngas compression train, the ammonia reactor, the waste heat recovery network, and the condensation and refrigeration systems. These units are interrelated to each other's operating conditions, affecting simultaneously the different sections of the flowsheet, as it is shown in Figure 1. Fresh syngas compressed above 150 bar is fed to the ammonia converter, where a nitrogen conversion between 10-30% is achieved in presence of a magnetite catalyst [28]. In order to achieve a higher ammonia conversion per pass, the reactor can be divided into three sequential catalyst beds with intercooling. The converter performance and, consequently, the loop efficiency, is affected by the reactor feed pressure, temperature and composition, as well as by the amount of inerts and ammonia recycled, the heat removal and catalyst design. Moreover, since ammonia condensation is not completely satisfactory by using only water or air cooling, the reactor effluent and fresh incoming gas must be refrigerated to about  $-20^{\circ}\text{C}$  in a two-stage R717 refrigeration system with intercooling.

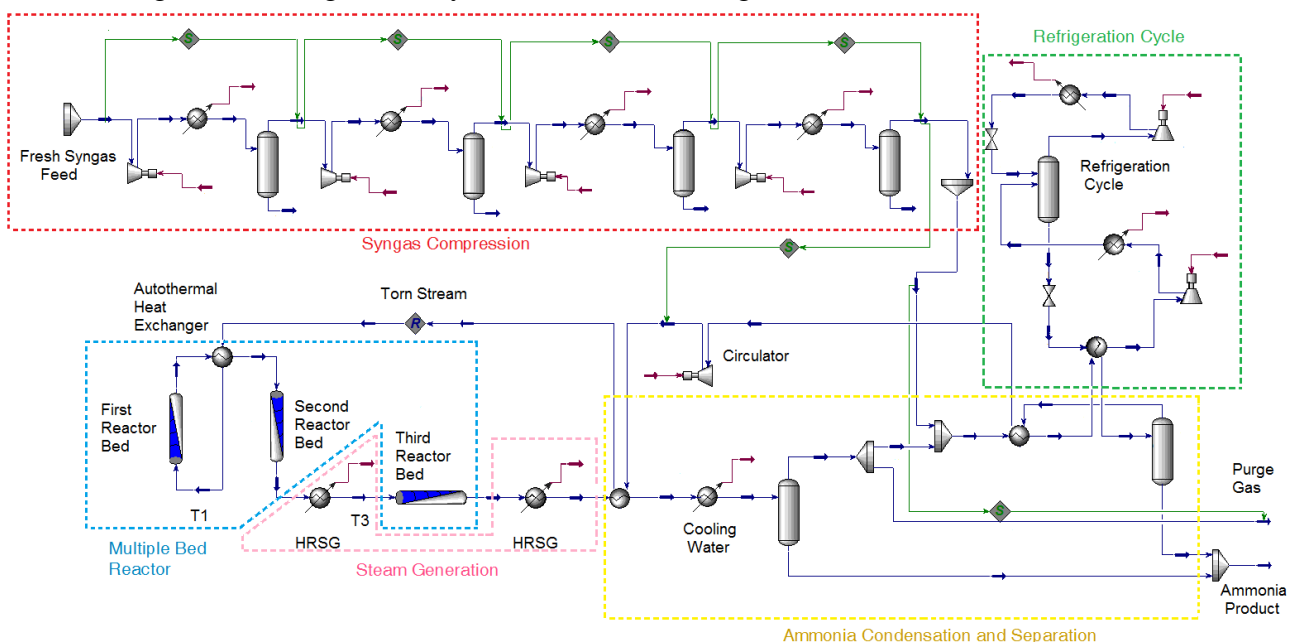


Fig. 1. Flowsheet of the ammonia production unit.

Additionally, the build-up of inerts (i.e., argon, methane, water) is controlled by a continuous withdrawal of a portion of the hydrogen-rich recycle gas to keep inerts concentration down to an acceptable level [29]. The best point for this withdrawal is where concentrations of inerts are higher, i.e., after ammonia bulk removal and before fresh syngas addition [30]. Among the advantages of the purge process are: (i) the removal of inerts from the ammonia loop without appreciable loss of

valuable hydrogen, (ii) the enhancement of the reactivity of the system, which in turn reduces the size of the equipment, (iii) the reduction of the power consumption in the syngas circulator and the refrigeration system [16]. In modern ammonia units, this valuable hydrogen is usually recovered from the purge gas and recycled to the synthesis loop [31].

### 3. Methodology

The exergy method is used to assess the performance of the various components of the ammonia production unit. In the following sections, the process balances, exergy efficiency definitions and the optimization methodology are presented.

#### 3.1. Process modeling

Mass, energy, exergy and economic balances of each sub-process under interest are carried out by the use of Aspen Hysys® V8.6 software. Since process streams in ammonia units are complex multi-component/multi-phase systems, an enhanced SRK equation of state (EOS) in Aspen Hysys® based on the semi-empirical EOS of Redlich-Kwong with Soave modifications (SRK), is used to determine the thermo-physical properties of each flow present in the system. The volume translation concept introduced by Peneloux et al. [32] is used to improve molar liquid volume calculated from the cubic equation of state [33]. Proprietary enhancements are claimed to allow SRK method to handle high pressure systems with an extended range of applicability. Some improved binary interaction parameters were used in order to obtain the species fugacities in both phases to accurately calculate the vapor-liquid equilibrium (VLE) of non-condensable species in liquid ammonia [34]. Moreover, as exergy calculation is not straightforward in the Aspen Hysys® environment, physical and chemical exergy calculations, as well as exergy efficiencies are assessed using VBA® scripts as *user defined functions* [35]. Aspen Hysys® is also used to assess the performance of the process components working under different loads and conditions, for predicting the energy demand of chemical processes and modeling systems involving complex chemistry, such as the ammonia reactor. Costs of the process streams and bare module equipment costs for the ammonia loop are calculated by using the methodology proposed by Turton et al. [36]. Finally, some indicators for estimating the performance of each configuration of the processing unit, which allow performing systematic comparisons between different designed setups, are proposed.

##### 3.1.1. Process kinetics and equilibrium conversion

By considering the stoichiometry of the ammonia synthesis reaction (R.1) in a packed bed reactor (PBR) operating at steady state:



the nitrogen mol balance in terms of the reactor conversion  $\xi$ , the catalyst volume  $V$  and the reaction rate  $r$ , is given by Eq.(1):

$$\xi = \frac{n_{N_2,inlet} - n_{N_2,outlet}}{n_{N_2,inlet}} \rightarrow n_{N_2,inlet} \frac{d\xi}{dV} = -r_{N_2} \quad (1)$$

where the rate of production or consumption of the other species is given by  $-r_{N_2}/1 = -r_{H_2}/3 = r_{NH_3}/2$ . The general Temkin-Phyzev expression, Eq.(2), which is consistent with the equilibrium constant, correlates the reaction rate of ammonia synthesis over a magnetite catalyst [37]:

$$-r_{N_2} = \frac{r_{NH_3}}{2} = k_b \left[ K_P^2 f_{N_2} \left( \frac{f_{H_2}^3}{f_{NH_3}^2} \right)^\alpha - \left( \frac{f_{NH_3}^2}{f_{H_2}^3} \right)^{1-\alpha} \right] \left[ \frac{kmol}{m_{cat}^3 \cdot h} \right] \quad (2)$$

According to the Lewis-Randall rule,  $f_i = x_i \cdot f_i^\circ$  is the fugacity of the component  $i$  at the partial pressure of the component in the system, and the equilibrium constant  $K_p^2 = k_f/k_b$  can be calculated as suggested by [38]. Based on proprietary catalyst data, some studies [39] have reported the pre-exponential factor and the activation energy for the backward ( $b$ ) reaction of ammonia synthesis, and those values are shown in Table 1.

Table 1. Pre-exponential factor and activation energy for backward ( $b$ ) reaction [39].

Parameter	$k_{0b}$	$E_{ab}$ (kJ/kmol)	$\alpha$	Observations
Value	2.57e14	163500	0.55	Montecatini catalyst, $f$ in atm.

This equation is aimed to predict the ammonia production rate with a maximum deviation of 10-20% within the pressure range of interest 150-300 atm. [39]. The pure component fugacity at the temperature and pressure of the system  $f_i^\circ$  is estimated by Eq.(3):

$$f_i^\circ = \gamma_i \cdot P \quad (3)$$

where  $\gamma_i$  is the activity coefficient of component  $i$  and  $P$  are total pressure of the reactive system. The activity coefficients are calculated as in Dyson and Simon [37]. The pressure drop along the reactor bed is fairly calculated by using Ergun correlation, Eq.(4) [40]:

$$\frac{dP}{dz} = -\frac{G}{\rho D_p} \cdot \frac{(1-\phi)}{\phi^3} \cdot \left[ \frac{150(1-\phi)\mu}{D_p} + 1.75G \right] \quad (4)$$

where  $\phi = V_{Gas}/V_{Bed}$  is the void fraction of the packed bed volume,  $\rho$  is the gas density,  $G = \dot{m}/A$  is the superficial mass velocity the reacting gases, and  $D_p$  is the catalyst effective diameter. Typical void fraction varies from 0.33 to 0.5 [41], with larger values requiring larger reactor volumes, and lower values leading to larger pressure drops. Furthermore, since each plug flow reactor bed is considered as adiabatic, the nitrogen conversion calculated at the bed outlet from the energy balance  $\xi_{EB}$  is given by Eq.(5) [40]:

$$\xi_{EB}^{Energy\ Balance} = \frac{\sum \Theta_i C_{p,i} (T - T_0)}{-[\Delta H_R^\circ(T_R) + \Delta C_p (T - T_R)]} \quad (5)$$

where  $\Theta_i = n_{i,inlet}/n_{N_2,inlet}$  is the ratio between the molar flow of the reactant  $i$  to the molar flow of the *inlet* nitrogen;  $C_{p,i}$  is the specific heat capacity of the *reactant*  $i$ ; and  $T$  and  $T_1$  are the product and reactant temperatures, respectively. The denominator corresponds to the reaction enthalpy at  $T$ , whereas  $T_R$  is the reference temperature used to calculate the enthalpy of reaction at the reference state (i.e. 298K and 1 atm). Equations (1-5) shall be simultaneously solved for the reactor design problem, and, thus, the nitrogen conversion calculated from the energy balance, Eq.(5), must be equal to that calculated from the molar balance, Eq.(1). Since the second term in the denominator of Eq.(5) is often negligible compared with  $\Delta H_R^\circ(T_R)$ , the operation curve of the adiabatic bed can be approximated by a linear function with a slope  $\beta \approx \sum \Theta_i C_{p,i} / -[\Delta H_R^\circ(T_R)]$  in a  $\xi$  vs.  $T$  plot (Fig. 2). Thus, the conversion at equilibrium corresponds to the intersection of the equilibrium curve ( $r_{N_2} = 0$ ) and the adiabatic operation line. It is noteworthy that, although Eq.(5) may resemble a means of calculating the conversion efficiency of the chemical energy into thermal energy (i.e., temperature increase) of the mixture, this definition requires the reaction enthalpy to be calculated for both reactor feed and effluent at the *outlet temperature*,  $T$ . Furthermore, the numerator of Eq.(5) is calculated from the properties of the molar flow going into the reactor bed only. Therefore, the reactor efficiency definition must not be mistaken with the nitrogen conversion definition given by

Eq.(5). Withal, it must be noted that both Eqs.(5) and exergy efficiency are related by the Second law of Thermodynamics, since an increase in the reactor conversion leads to an increase of the reactor irreversibilities, and thus, a decrease in the exergy efficiency of the reactor bed. Figure 2 also shows the *locus of maximum conversion*, defined as the set of temperatures at which the maximum conversion is achieved for a given reaction rate. It would be therefore advantageous to operate near this line so that catalyst volumes would be reduced. However, for adiabatic reactors, the maximum reaction rate obtained inside the bed is rather in the tangency points between the adiabatic operation line and the lines of constant reaction rate.

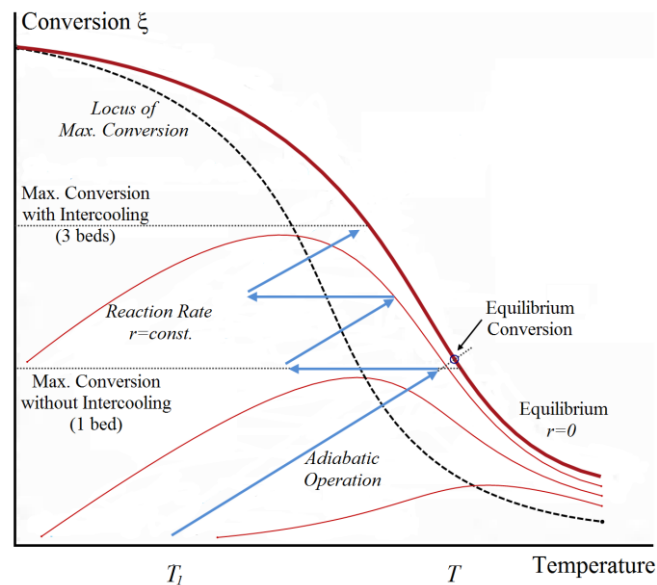


Fig. 2. Adiabatic operation lines, reaction rate contours and maximum conversion in an exothermic reactor [40].

In this work, it is assumed that the effectiveness factor of the small catalyst particles used (3 mm, bulk density 2300 kg/m<sup>3</sup>, sphericity 1) is close to the unity, thus the reactants concentration inside the particles is close to the bulk concentration. The reactor nominal volume is calculated by considering a packed bed reactor (in contrast to industrial non-circular cross-sectional configurations) and is assumed that the axial diffusion effect diminishes with the increase of the flow rate in the channel. In other words, the model is simplified to a packed bed reactor (PBR) in Aspen Hysys® with a very fast radial mass transport and a large ratio of reactor-to-pellet diameter. The flow is assumed turbulent so that the rapid mixing of reactants is guaranteed. A more detailed resolution of the reactor simulation would be obtained by coupling the modeling of the non-linear reaction kinetics to the computational fluid dynamics, which would considerably increase the computational time without an appreciable variation of the whole loop results. Thus, a trade-off between the effect of the reactor performance and reasonable computational time frames is selected. Additionally, the effect of the catalyst aging in its activity variation remains out of the scope of this paper. Finally, at up to moderated pressures, the vapor-liquid equilibrium (VLE) of ammonia could be estimated by applying Raoult's law and considering that condensed ammonia is almost pure in the liquid phase (i.e. ideal solution), whereas the ammonia in equilibrium in the vapor behaves as in an ideal mixture of non-ideal gases [42]. However, for higher pressures and for species above their critical temperatures, the fugacity of the species  $i$  in the non-ideal liquid phase is more conveniently calculated in terms of the system pressure  $f_i = x_i \cdot \phi'_i \cdot P$  (instead of in terms of their vapor pressure  $f_i = x_i \cdot \gamma_i \cdot p_i$ ), especially for substances whose vapor pressure  $p_i$  may not be defined above their critical temperatures (such as dissolved hydrogen). The fugacity coefficient of species  $i$ ,  $\phi'_i$ , in both

liquid ( $x_i$ ) and vapor ( $y_i$ ) phases is thus computed from the same equation of state (EOS), as well as the other thermodynamic properties such as densities, enthalpies and heat capacities [42].

### 3.1.2. Exergy calculation and exergy efficiency definition

The combination of the first two Laws of Thermodynamics led to the concept of *exergy*, which is defined as the maximum work that can be obtained by means of reversible processes from a thermodynamic system that interacts with the components of the environment until the dead state equilibrium is attained [43]. The environmental parameters are assumed as  $P_0 = 1\text{atm}$ ,  $T_0 = 298.15\text{ K}$ . Since exergy can be considered as a measure of the departure of the environmental conditions, it serves not only for defining indicators to assess the performance of chemical processes, but also as an indicator of environmental impact. The total exergy can be divided into potential (P), kinetic (K), physical (PH) and chemical (CH) components, Eqs. (6-7) [43]:

$$B^{PH} = H - H_0 - T_0(S - S_0) \quad (6)$$

$$B^{CH} = N_{mix} \bar{b}^{CH} = N_{mix} \left[ \sum_i y_i b_i^{CH} + R_u T_0 \sum_i y_i \ln \gamma_i y_i \right] \quad (7)$$

Where  $y_i$  and  $\gamma_i$  are the mole fraction and the activity coefficient of component  $i$  in the mixture, respectively, and  $b_i^{CH}$  is the standard chemical exergy of component  $i$ . The exergy balance of a control volume in steady state operating conditions is given by Eq.(8):

$$\sum B_{in}^M - \sum B_{out}^M + \sum B_{in}^Q - \sum B_{out}^Q + \sum W_{in} - \sum W_{out} = B_{Dest} \quad (8)$$

where  $B^M$ ,  $B^Q$  and  $W$  are the exergy associated to the mass, and the heat and work interactions, respectively; and  $B_{Dest}$  stands for the exergy destruction due to the irreversibilities in the system.

#### 3.1.2.1 Exergy efficiency of ammonia loop: Two novel definitions.

Due to the large recycle rates and low conversions in ammonia synthesis loop, the proposition of a global definition of exergy efficiency for the ammonia loop is not straightforward. In this work, two types (i) *input-output* and (ii) *consumed-produced* exergy efficiencies are evaluated. The first type, which considers the ratio between all the exergy flows leaving the system and the exergy flows fed to it, may provide misleading results as its sensitivity deceptively reduces with the amount of untransformed components. The second type attempts to differentiate the exergy effectively transformed by the system from the untransformed exergy, by calculating the exergy change of specific streams on the way to product.

Notwithstanding its simple formulation, the *input-output* exergy efficiency, defined by Szargut et al. [43] as in Eq.(9), may provide misleading results as it deceptively assumes values close to unity for operations which, from an engineering point of view, have a poor performance [44, 45]. *Input-output* type efficiency can be even negative for some process [46]. Table 2 compares an *input-output* type, namely the rational exergy efficiency, Eq. (9), along with several exergy efficiency definitions, Eqs.(10-12), proposed for better evaluating the overall performance of the ammonia loop [1]. Since the exergies of the input and output material flows are much larger than the energy flows (i.e, the power consumption), the rational exergy efficiency leads to untruthfully high and similar values. To overcome this, an alternative approach has been proposed first by Kirova-Yordanova [12], where the useful exergy of the material output is considered as *transit exergy*, subtracting it from the numerator and denominator of Eq.(10), Table 2. However, Eq.(10) must be used with care, since it considers that all the outlet material flow is exergy in transit, although a chemical reaction of the syngas occurs in the loop. Actually, according to Brodyansky et al. [47] only inerts could be regarded as *transit exergy* [46]. Equation (10) also assumes that all the non-

reacted nitrogen and hydrogen is recycled back to the ammonia converter and thus liquid ammonia, methane and argon are the only material exiting the system.

Table 2. Comparison among the exergy efficiency definitions of the overall ammonia synthesis unit.

Definition	Formula
Rational (9)	$\eta_{\text{Rational}} = \frac{B_{\text{useful,output}}}{B_{\text{input}}} = 1 - \frac{B_{\text{Dest}}}{B_{\text{input}}} = 1 - \frac{B_{\text{Dest}}}{\left( B_{\text{Makeup Syngas}} + B_{\text{BFW}}^{\text{PH}} + W_{\text{Total}} \right)}$
Transit (10)	$\eta_{\text{Transit}} = \frac{\left( B_{\text{useful,output}}^{\text{Total}} - B_{\text{useful,output}}^{\text{Material}} \right)}{\left( B_{\text{input}}^{\text{Material}} - B_{\text{useful,output}}^{\text{Material}} + B_{\text{input}}^{\text{Exergy Flow}} \right)} = \frac{B_{\text{Steam}}^{\text{PH}}}{\left( B_{\text{Makeup Syngas}} + B_{\text{BFW}}^{\text{PH}} - \left[ B_{\text{Ammonia}} + B_{\text{Inerts}} \right] + W_{\text{Total}} \right)}$
Recovered (11)	$\eta_{\text{Recovered}} = \frac{B_{\text{Recovered}}}{B_{\text{Consumed}}} = \frac{\left( B_{\text{Steam}}^{\text{PH}} - B_{\text{BFW}}^{\text{PH}} \right)}{\left( B_{\text{Makeup Syngas}} - \left[ B_{\text{Ammonia}} + B_{\text{OffGas}} \right] + W_{\text{Total}} \right)}$
Relative (12)	$\eta_{\text{Relative}} = \frac{B_{\text{Consumed, ideal}}}{B_{\text{Consumed, actual}}} = \frac{B_{\text{Ammonia}}}{B_{\text{Makeup Syngas}} + B_{\text{BFW}} + W_{\text{Total}}}$

Due to the shortcomings of the previous exergy definitions and by considering the process technical limitations and the exothermic characteristics thereof (e.g. need for intercooling, kinetics, etc.) [48], in this work, a more appropriate way to calculate the loop performance is proposed. Since the reaction enthalpy of ammonia synthesis is about 8.8% (2.718 MJ/t<sub>NH3</sub>) of the total consumption in the integrated syngas-ammonia plant, there is a strong incentive in recovering as much as possible of this surplus heat [28]. In fact, the mass of steam consumed even in advanced units is 3-4 times higher than ammonia produced [49]. Steam is used (i) to drive pumps and gas compressors, (ii) reboilers and (iii) as feedstock primary reformers. Accordingly, by considering an *ideal* case in which all of the exergy input neither embodied in the ammonia nor in the off-gas products is recovered in the form of steam (see Eq.(13)), a new efficiency definition, Eq.(11), Table 2, can be proposed [1]:

$$B_{\text{Dest}} = 0 \rightarrow B_{\text{Steam}} = B_{\text{Fresh Syngas}} - \left[ B_{\text{Ammonia}} + B_{\text{Purge}} \right] + W_{\text{Compressor}} + W_{\text{Circulator}}^0 + W_{\text{Refrigerator}} + B_{\text{BFW}} \quad (13)$$

Eq.(11) impose a limit for the maximum exergy recovery in the form of steam, when pressure drop ( $W_{\text{Circulator}} \rightarrow 0$ ) and process irreversibility ( $B_{\text{Dest}} \rightarrow 0$ ) tends to zero. Since the exergy difference and not the total mass flows are written in Eq.(11), the difficulties presented when defining the exergy efficiency of large recycle systems can be overcome. On the other hand, Eq.(11) is evaluated in terms of the exergy recovery potential. However, by realizing that the main objective of the chemical unit would be rather to produce ammonia, instead of expending the valuable incoming exergy of the makeup syngas in producing lower quality exergy of steam, in this work, a second exergy efficiency definition is introduced. Equation (12) is calculated as the ratio of the minimum exergy consumption in ammonia production (i.e. the ammonia chemical exergy, 327,000kJ/kmol) to the actual loop consumption. Since the denominator of Eq.(12) includes the exergy of the material flow rate of the makeup syngas, this definition is slightly less sensitive to the loop parameters, such as recycle/purge ratio, refrigeration duty and pressure drop, all of them represented by the total power consumption term. Anyhow, Eq.(12) gives a measure of the overall potential of improvement of the loop when compared with the minimum exergy requirements for ammonia production from nitrogen and hydrogen. It is clear that this value can be much lower if the boundaries of the system are extended for including, for example, the front-end syngas production process.



Table 3 compares the proposed exergy efficiency definitions for representative components of the ammonia unit against the widely used *rational* efficiencies. In Eq.(14), the exothermic ammonia converter efficiency is defined in terms of the increase of thermal exergy of the reactor effluent at the expense of a fraction of the chemical exergy of the reactants [11].

Table 3. Exergy efficiency definitions for representative equipment.

Unit (Eq.)	(a) Input-Output	(b) Consumed-Produced
Syngas Compression (14)	$\eta_{Comp,IO} = 1 - \frac{B_{Dest, Comp}}{\left( B_{Fresh\ Syngas}^{Tot} + W_{Comp} + W_{Cooling\ Tower} \right)}$	$\eta_{Comp,CP} = \frac{\left( B_{Compressed\ Syngas}^{PH} - B_{Makeup\ Syngas}^{PH} \right)}{W_{Comp} + W_{Cooling\ Tower}}$
Ammonia Reactor (15)	$\eta_{Reactor,IO} = 1 - \frac{B_{Dest, Reactor}}{B_{Reactor\ Feed}^{Tot}}$	$\eta_{Reactor,CP} = \frac{B_{Reactor\ Product}^{PH} - B_{Reactor\ Feed}^{PH}}{\left( B_{Reactor\ Feed}^{CH} - B_{Reactor\ Product}^{CH} \right)}$
Refrigeration cycle (16)	$\eta_{Refrig,IO} = 1 - \frac{B_{Dest, Refrig}}{W_{Comp\ I} + W_{Comp\ II} + W_{Cooling\ Tower} + B_{Evap}^Q}$	$\eta_{Refrig,CP} = \frac{-Q_{Evap} (T_0/T_{Evap} - 1)}{W_{Comp\ I} + W_{Comp\ II} + W_{Cooling\ Tower}} = \frac{COP_{actual}}{COP_{Carnot}}$ $\eta_{Refrig,CP2} = \frac{B_{Syngas,in}^{PH} - B_{Syngas,out}^{PH}}{W_{Comp\ I} + W_{Comp\ II} + W_{Cooling\ Tower}}$
Waste Heat Boiler (17)	$\eta_{HRSG,IO} = 1 - \frac{B_{Dest, HRSG}}{\left( B_{Hot\ Gas}^{Tot} + B_{BFW}^{Tot} \right)}$	$\eta_{HRSG,CP} = \frac{\left( B_{Steam}^{PH} - B_{BFW}^{PH} \right)}{\left( B_{Hot\ Gas}^{PH} - B_{Cold\ Gas}^{PH} \right)}$

Here, the increase (or decrease) of the chemical exergy of specific input and output streams going through the unit is considered as a first contribution to the exergy product (or consumption) of the respective unit. Similarly, the increase (or decrease) of the physical exergy of the product compared to that of the feed is regarded as a useful exergy output (or expenditure). Other contributions such as power and heat interactions are also accounted for as produced or consumed exergy rates when necessary. In Eq.(17), two approaches are considered for the refrigeration cycle. Differently from the first approach (CP), the second efficiency (CP2) includes the irreversibilities in the control volume of the evaporator, thus  $B_{Process\ Gas}^{PH}$  stand for both the inlet and outlet refrigerated process gas.

### 3.2. Optimization problem definition

The ammonia synthesis is an interesting application for evaluating the limitations on the parametric optimization of exothermic (equilibrium-limited) processes at high temperatures and pressures that present recycle/purge streams. The interrelation between the inlet temperature, reaction kinetics and catalytic beds arrangement and its effects in the performance of the ammonia condensation and heat recovery network are thus determined. Figure 2 reveals two conflicting effects that arise in the operation of exothermic reactors [50]. First, when the reaction starts far away from equilibrium ( $T = T_1$ ), the kinetics is favored by a temperature increase and, thus, the conversion increases. But also, since the maximum attainable conversion ( $r=0$ ) decreases by increasing the temperature, the rate of reaction diminishes on approaching equilibrium and, eventually, the conversion falls [51, 52]. Even if, for a given temperature, the maximum conversion is attained at the thermodynamic equilibrium, close approaches would require large volumes of catalyst. Thus, in order to shift the mixture away from equilibrium and increase per-pass conversion, a multi-bed ammonia reactor with intercooling is preferred [16, 53]. Moreover, indirect instead of direct (quenching) intercooling is adopted [54], since it allows increasing the ammonia yield (by preheating the reactor feed stream) and simultaneously integrating the steam network to the chemical plant [16, 28]. Larger throughputs can also be achieved by purposely increasing the operating space velocity (i.e. ratio of volumetric flow rate to catalyst volume), although it may also lead to a reduction in the per-pass conversion

[16, 54, 55]. These enhancing techniques deal with the Le Chatelier Principle, which attempts to increase the ammonia production by increase the reacting driving force [56].

However, by continuously shifting the reaction away from equilibrium, not only the ammonia yield but also the irreversibilities of the system (i.e. the destroyed exergy) are increased, reducing the loop efficiency and also increasing the utilities demand [11]. Thus, aiming to reduce the avoidable exergy losses, it would be desirable to apply a “counteraction” that reduces the driving force of the chemical process ( $-\Delta G$ ), either by increasing the temperature of exothermic reactions or by reducing the pressure of decreasing-volume reactions (Counteraction Principle) [11]. Accordingly, in this work, by considering that the capital costs are nearly constant for a given operating pressure in a 1000 metric t/day ammonia unit, the *minimization of the exergy destroyed per unit of exergy of useful product* is adopted as a suitable optimization criterion to determine the rational approach-to-equilibrium and the extent at which the reactive mixture must be cooled down before going to the subsequent bed [23, 57]. Since the simulation of chemical processes involving reactor-separation-recycle systems are likely to present convergence issues because of the *snowball effect* in the recycle stream [56], appropriate initial guesses for the properties of the torn stream are required. Also, advanced acceleration methods (*dominant-eigenvalue*) are preferred over inefficient successive substitution. In this work, a sequential quadratic programming (SQP) tool in Aspen® Hysys is used to solve the optimization problem described in Table 4.

Table 4. Optimization problem definition.

<p><b>Objective function:</b> Exergy destruction minimization.</p> <p><b>Subject to the constraints:</b></p> <ul style="list-style-type: none"> <li>• Minimum temperature approach at the autothermal heat exchanger: the heat of reaction of the first bed must be enough to raise the temperature of the incoming gas without further addition of heat.</li> <li>• Minimum temperature approach in the waste heat recovery exchangers. Avoid temperature cross between the process gas and steam.</li> <li>• Convergence of the recycle tearing.</li> <li>• Composition of inerts (&lt; 15.4%) and ammonia (&lt; 2.6%) in the recycle gas are kept to low levels.</li> <li>• For hydrogen safe operation, max. loop temperatures limited to 530°C. Metallurgical limitations at high pressure, adverse effects on catalyst activity and lifespan.</li> <li>• The risk of poisoning by even low O<sub>2</sub> concentrations sets a practical lower bound to the catalyst temperature (290°C).</li> </ul> <p><b>Design Variables:</b></p> <ul style="list-style-type: none"> <li>• Preheating temperature of the feed gas going to the first bed, T<sub>1</sub> (290-500°C).</li> <li>• Intercooling temperature of the feed gas going to the third bed, T<sub>3</sub> (290-420°C).</li> <li>• Fresh syngas molar composition (Fresh syngas H<sub>2</sub>/N<sub>2</sub> ratio).</li> <li>• Loop pressure (150 bar, 200 bar).</li> </ul> <p><b>Constants:</b></p> <ul style="list-style-type: none"> <li>• For both 150 and 200 bar, reactor volume 1° bed: 29.4m<sup>3</sup>; 2° bed: 29.4m<sup>3</sup>; 3° bed: 39.3m<sup>3</sup>.</li> <li>• Reactor void fraction 0.46 [24, 58]. Catalyst effective diameter 3mm. Catalyst bulk density 2300 kg/m<sup>3</sup></li> <li>• Circulator and refrigerator compression efficiencies (75%).</li> <li>• Ammonia production rate (1000 metric t/day nominal).</li> <li>• Cooling water and boiler feedwater temperatures.</li> <li>• The diffusion and hydrodynamics effects are neglected.</li> </ul>
---

## 4. Results and discussion

In this section, the performance of two ammonia units, one operating at selected base-cases and the other at calculated optimal operation conditions are compared in terms of the exergy consumption, the reactor conversion, the exergy efficiency and exergy destruction in the various units.

### 4.1. Base-case and optimal operation conditions

Table 5 summarizes the process variables defined for the base-case unit and those calculated for the optimal unit operation conditions, according to the optimization problem given in Table 4. It is

worthy to notice that for both base-case operation pressures, a higher temperature  $T_1$  has been purposely selected promoting a counteraction effect that aims to reduce the irreversibilities in the highly exothermic ammonia reactor. Meanwhile, a low temperature  $T_3$  is chosen, so that, as the ammonia conversion progresses, the reacting driving force in the last reactor bed is reduced. It is interesting, however, that even if, as it will be shown, this approach allows reducing the share of exergy destruction in the reactor, when the base-case operation figures are compared with the optimal ones, the power consumption is considerably increased in the former cases. As it will be explained along this work, the observed behavior obeys a more complex relation between the different components of the ammonia unit. In fact, for the operating condition of 150 bar (SP150), the refrigeration power consumption in the base-case is about 69% higher, whereas the circulator power is at least 5.1 times greater than in the optimal case. This is a direct consequence of a high recycle rate, which reduces the reactor conversion in about 40%. For the base-case at 200 bar (SP200), the refrigeration power consumption is as much as 189% higher compared to the optimal case, whereas the circulator power is 28.2 times greater. Moreover, the reactor conversion is reduced in about 79%. On the other hand, it is observed that, for each operating pressure, similar water requirements are required in the water cooled heat exchanger; however, largest figures occur in the refrigerator condenser for the base-case conditions. Cooling water consumption is reduced by increasing loop pressure and reducing the recirculation flow rate.

For the SP150 and SP200 optimal setups, the syngas compression consumes almost 61% and 75% of the power supply, respectively, followed by the ammonia refrigeration cycle (36% and 24%) and the circulator. Contrarily, the refrigeration and syngas compression power consumptions are comparable for each base-case setup. It is important to notice that the total power consumption is similar for both optimal cases (approx. 13 MW). In fact, even if at the best case of SP200 lower amounts of ammonia and inerts recycled to the reactor are obtained (which reduces the recycle molar flow rate, the refrigeration and the circulator power consumptions), it is due to the 21.5% higher fresh syngas compression power required by the best case of SP200 which renders the low pressure optimal case of SP150 still competitive in terms of both power consumption (only 3.1% higher) and economic revenues (Table 5). Also, the highest exergy consumption corresponds to the base-case of SP200 (21.9 MW), whereas base-case operation of SP150 bar consumes about 18.9 MW. Given the compressor and circulator efficiencies and the loop pressure drop, some authors reported that a pressure-independent power consumption is obtained for operating pressures between 140–315 bar, with a flat minimum in 155 bar [59]. Other studies have found higher values (180–220 bar) [49]. However, those results should be interpreted with care since they are dependent on assumed conditions on catalyst activity, inlet and outlet equilibrium temperatures of each bed. Those studies also ignore the contribution of both the steam production and its impact on the whole exergy balance, as well as of the front-end fresh syngas pressure [49]. Accordingly, in the subsequent sections it will be shown that the selection of non-optimal reaction temperatures, pressure and compositions may radically increase the loop inefficiencies, thus increasing the power consumption.

Table 5. Main process variables in the selected base-case and calculated optimal unit operation conditions (1000 metric ton per day ammonia unit)

Process parameter	150 bar		200 bar	
	Base-case	Optimal	Base-case	Optimal
First bed gas preheating temperature, $T_1$ (°C)	450	365	410	310
Third bed inlet gas temperature, $T_3$ (°C)	340	400	340	380
Reactor pressure drop (bar)	10.7	3.5	16.2	1.5
Fresh syngas $H_2/N_2$ ratio	2.97	2.99	2.83	2.94
Fresh syngas inerts content (%)	1.25	1.27	1.10	1.22
Recycle ammonia content (%)	2.38	2.23	2.58	1.90

Process parameter	150 bar		200 bar	
	Base-case	Optimal	Base-case	Optimal
Recycle inerts content (%)	13.55	11.40	15.40	8.43
Recycled reactor feed H <sub>2</sub> /N <sub>2</sub> ratio	2.50	2.89	0.65	2.39
Recycle molar flow rate (kmol/h)	34,642	20,889	37,998	15,118
Fresh syngas compression power (kW)	8,140	8,140	9,890	9,890
Refrigeration power consumption (kW) <sup>1</sup>	8,267	4,883	8,996	3,104
COP Carnot	4.42	4.42	4.42	4.42
COP actual	2.43	2.43	2.43	2.43
Circulator power consumption (kW)	2,475	489	3,048	108
Purge gas fraction (%) <sup>2</sup>	7.0	7.0	7.0	7.0
First bed conversion (%)	10.9	17.5	5.1	20.7
Second bed conversion (%)	2.3	6.0	0.8	6.5
Third bed conversion (%)	2.4	5.8	1.0	7.2
Reactor conversion (%)	15.0	24.9	6.7	31.2
Waste heat recovery rate (kW) <sup>3</sup>	22,870	27,826	20,686	28,622
Cooling water - gas condensation (kmol/h) <sup>4</sup>	27,825	28,171	33,609	34,561
Cooling water – refrigeration cycle (kmol/h) <sup>4</sup>	555,351	328,029	604,318	208,476
Incomes (\$/ton NH <sub>3</sub> ) <sup>5</sup>	642.1	649.4	626.1	649.2
Costs (\$/ton NH <sub>3</sub> ) <sup>6</sup>	472.1	417.3	440.4	416.6
Revenues (\$/ton NH <sub>3</sub> )	169.9	232.1	185.6	232.6
Annualized Bare Module Cost (\$/ton NH <sub>3</sub> ) <sup>7</sup>	73.2	24.1	51.0	26.9

1. Condenser pressure: 13.6 bar, evaporator pressure: 115.2 kPa. Minimum temperature approach: 5-10°C; 2. As a constant fraction of the total molar flow of the fresh syngas (makeup); 3. Saturated steam as 100bar; 4. Cooling water maximum outlet temperature: 35-40°C; 5. Ammonia price: \$32/GJ; 6. Natural gas cost: \$9.7/GJ. Annualized bare module cost included; 7. Interest rate 6%, lifespan 20 years. CEPCI: 550 (2010) [14, 36].

Table 5 also shows that if the circulation rate is increased at constant loop pressure and ammonia production rate, a lower ammonia conversion is obtained, with a subsequent depart from the equilibrium and an increase the reaction rate [16]. At some extent, this may result in a lesser amount of catalyst required but, in this work, the catalyst bed volume is set as constant. In fact, higher recycled flow rates are rather advantageous when an increase of ammonia plant capacity is aimed to [55]. It must be also noted that, due to an increased circulation rate in the base-case conditions, a higher amount of ammonia is recycled to the reactor, eventually hindering further ammonia production. Thus, lower separation temperatures would be necessary if smaller amounts of recycled ammonia in the reactor feed are aimed to [59]. On the other hand, since the level of temperature of waste heat recovery also decreases with a higher recycle rate, larger heat exchanger areas and piping sections are required to account for increased flows, and also higher power consumptions are needed to overcome higher pressure drops. Finally, with higher space velocities, larger separation vessels are required for appropriate residence times of the separating mixture, increasing so the capital costs. In this way, due to the increased utilities consumption, lower revenues are achieved when operating under the selected base-case conditions, even if they are in agreement with the counteraction principle applied to the reactor alone. Obtained cost values are in agreement with those reported for natural gas based ammonia plants [14].

## 4.2. Reaction kinetics in the multi-bed catalytic reactor with intercooling

Figure 3(a-d) are graphical representations of the relation between the kinetics operation parameters of the multi-bed catalytic reactor (e.g, bed feed temperature, conversion and reaction rate) and the indirect cooling system. They correspond to the kinetics properties of the Montecatini catalyst reported in Table 1. The contours of constant reaction rates, equilibrium and adiabatic operation

lines have been determined for each one of the operating conditions, reported in Table 5. As it can be observed, due to the interrelated recycle, conversion and separation aspects, a slight deviation from the stoichiometric  $H_2/N_2$  ratio in the fresh (makeup) syngas fed to the ammonia loop may develop into an appreciable difference from this ratio in the converter feed stream [60]. This is purposely represented in the non-optimal case shown in Fig.3(c), in which a low reactor conversion and a large recycle rate are responsible for a striking reduction of the calculated  $H_2/N_2$  ratio at the recycled reactor feed ( $\sim 1$ ). Despite extremely low  $H_2/N_2$  operation ratios may not immediately represent practical applications, they are interesting for analyzing the effect of the variation of some loop parameters (particularly the reactor feed temperature) on the feasible window of the operating conditions, as it will be shown in section 4.4. According to Fig. 3(c), as the departure from equilibrium and, therefore, the reaction rate, is increased, the reaction heat available and, consequently, the temperature of the reactor effluent is reduced, affecting the performance of the autothermal heat recovery and the conversion in the second lined reactor bed. This represents a thermodynamically and kinetically feasible scenario, but also an extreme operation condition in which the minimum temperature approach constraint in the reactor bed intercooler is almost violated. For instance, some studies [16] reported a marked dependence of the reaction rate on the ratio of the hydrogen and nitrogen content, with the maximum rate shifting to a lower  $H_2/N_2$  ratio at lower temperatures. Moreover, a sharper drop in reaction rate is reported to occur at a  $H_2/N_2$  ratio of 3:1, with declining temperature, in contrast to a 1:1 ratio, which has been attributed to a hindering effect of absorbed hydrogen at low temperature [16]. Thus, for a fixed catalyst volume, the decision-making on the optimum reactor feed and effluent temperatures would require a trade-off between the approach to and the shifting away from equilibrium line [28].

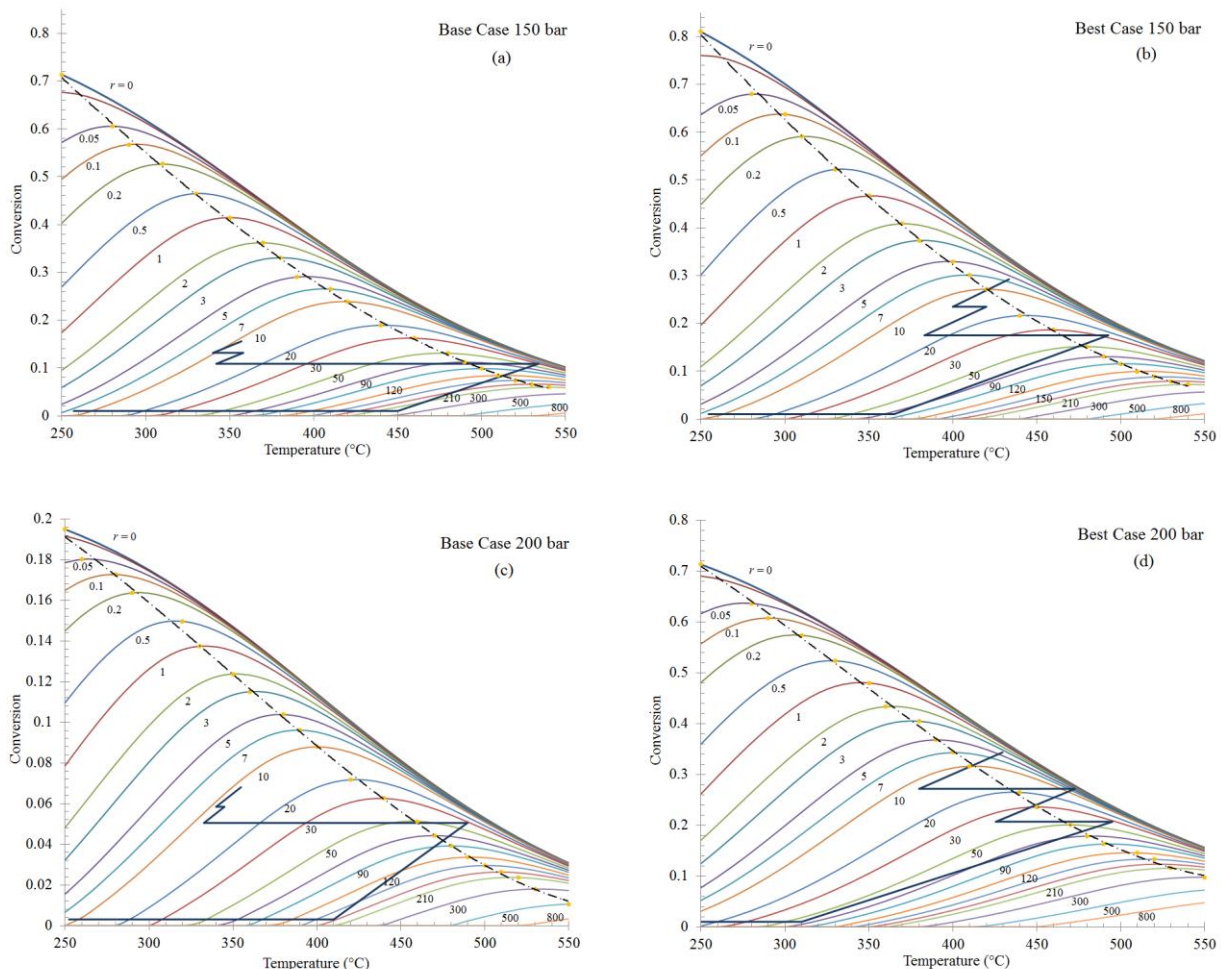


Fig. 3. Conversion vs. Temperature. (a) Base-case 150 bar, (b) Optimal operation 150 bar, (c) Base-case 200 bar, (d) Optimal operation 200 bar. Reaction rates are given in  $kmol/m^3 \cdot h$ .

The curve along which all the points of maximum conversion occur is called the “*locus of maximum conversions*” [52] and can be determined by solving the Eq.(18):

$$\left. \frac{dr_{N_2}}{dT} \right|_{\xi=\text{constant}} = 0 \quad (18)$$

The *locus of maximum conversion* entails the existence of a point of minimum recycle flow rate for a *fixed catalyst volume*. It is observed that, differently from the base-case operation conditions, the optimal temperature profiles are allocated at both sides of the line of maximum conversion, although simultaneously avoiding a narrow approach to the *equilibrium curve*, which appears shifted 30-70°C to the right of the former line [50, 51]. It must be also noted that, the lower the pressure, the lower the feed temperatures required for a reasonable conversion, since the equilibrium curve ( $r = 0$ ) is shifted to the left [59]. An important conclusion drawn from the performance of the optimal setups is that, even though the reacting driving force is still increased, the performance expected by the Counteraction principle is not the same for a standalone reactor when it is linked to the performance of other surrounding thermal systems. Thus, the Counteraction principle and Le Chatelier principle do not necessarily represent irreconcilable concepts derived from the Second Law. As it is shown here, the increase of the reacting driving forces in the ammonia converter does not always lead to increased whole system irreversibilities, since the global effect of the finite driving forces in that equipment may be compensated by the enhancement of the performance of the integrated chemical unit (enhanced power consumption, cooling duty, recycle composition, equipment sizing, etc.). Conversely, optimal operation conditions for the ammonia loop as a whole do not necessarily correspond to an optimal operation condition of the ammonia reactor alone [9, 28, 45, 61]. This is a characteristic of highly non-linear systems in which multiple changes that individually are detrimental may lead to much improved performances when combined [62].

Higher conversions could be also achieved if more active catalysts at lower pressures (~ 80 bar) and temperatures were used [18]. Among them, the ruthenium catalyst used in the Kellogg Advanced Ammonia Process (KAAP) is claimed to be 10-20 times more active than conventional iron-based catalyst, which are simultaneously used in the Haldor Topsoe S300 ammonia converter layout. Energy savings of about 1.17 GJ/ton<sub>NH<sub>3</sub></sub> have been reported [28, 54]. According to this, the overall reactor performance could be enhanced by using a set of suitable catalysts along the reactor beds. However, this improvement again poses detrimental effects on the overall unit integration. For instance, if ammonia synthesis is carried out at 200°C, this low grade temperature reactor effluent is not anymore available for high pressure steam generation [27]. On the other hand, the benefits would be related to the reduction of the compression power and the cost reduction of the equipment involved (i.e., increasing its safety and reliability). Thus, every time a radical development is envisaged, the front-end syngas plant integration must be thoughtfully considered. It would also be desirable to perform the reaction under *resisted conditions* [48], so that the chemical exergy can be maximally exploited. Unfortunately, this is a practical shortcoming in large-scale industrial applications, because it would require slow enough, quasi-reversible conditions [23] or strict coupling between thermal and chemical forces of the system which is not always feasible [63].

### 4.3. Exergy destruction and Efficiency of representative equipment

Since real processes are based on finite-driving forces, they are necessarily irreversible, and a portion of the exergy is always destroyed as the system evolves towards equilibrium. Exergy destruction accounts for the system inefficiencies and gives a useful measure of the way in which the resources are consumed and degraded. However, *exergy losses* are not always inevitable and, in some cases, a portion of them may be avoided if optimal operation conditions are adopted. In other words, the *exergy analysis* provides a valuable tool that allows comparing the actual and the ideal performance, limiting the technological developments to feasible solutions. Figures 4 and 5 show

the exergy destruction figures and the exergy destruction breakdown, respectively, calculated for the most representative components of the ammonia loop. In the following, the exergy performance and suitable alternatives for improving the exergy efficiencies are discussed.

For the standalone reactor system, the exergy inlet associated with unreacted feed or inerts typically constitutes transiting exergy [44]; however, its impairing effect on the whole ammonia loop is evident. In fact, due to the large recycle rates and lower per-pass conversions, the exergy destruction in the ammonia reactor is higher than other industrial exothermic reactors [64, 65]. But, despite the fact that most of the irreversibility due to chemical conversion is inevitable, some exergy losses can still be reduced if the heat transfer irreversibilities are reduced (reactants preheating) and the reactor pressure is increased [43]. A beneficial point of the pressure increase would be the potential reduction of the power consumption in the circulator and the refrigeration systems, but at expense of a higher exergy consumed in the syngas compressor train. In order to deal with this problem, novel dual pressure ammonia loops (e.g. Udhe process), that operates by starting at lower pressures and proceeds at higher ones, aim to reduce the syngas compression duty but maintaining high production rates [31]. It is important to notice from Fig. 5, that the exergy destruction share of the reactor is effectively reduced when a counteraction is applied to the driving forces. Thus, even though the reduction of the local exergy destruction share is obtained, the interaction of the energy systems dictates the actual optimal operating condition of the standalone components.

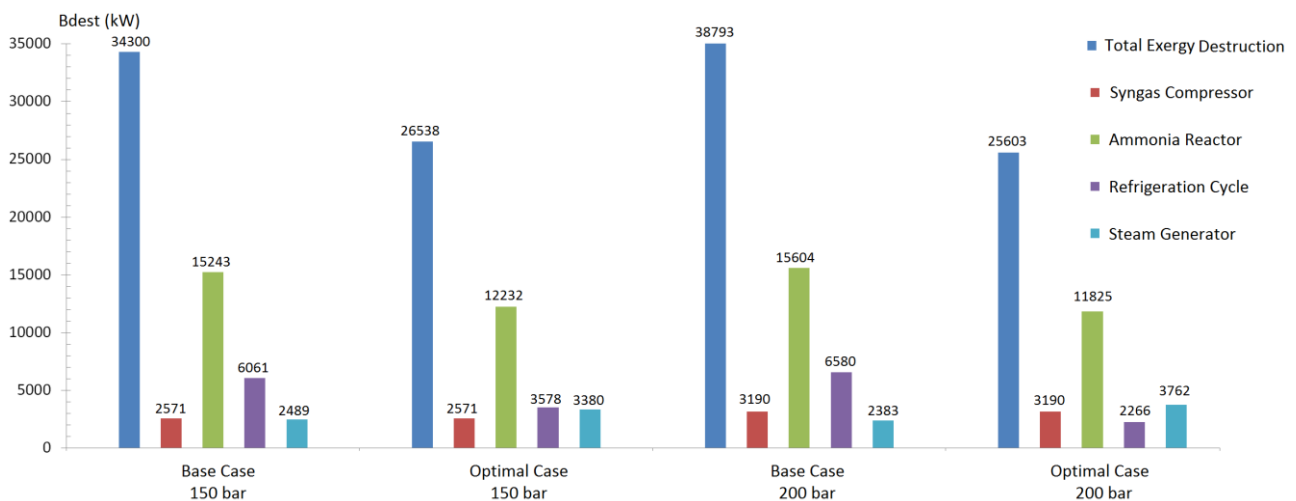


Fig. 4. Exergy destruction of representative components of the ammonia loop.

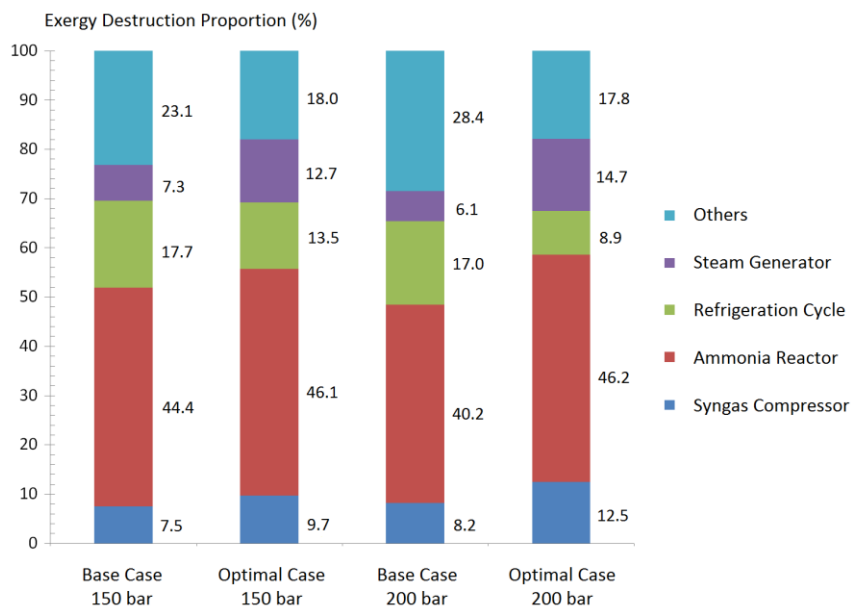


Fig. 5. Exergy destruction breakdown for representative components of the ammonia loop.

Some authors proposed the expansion of the reactor effluent in ammonia expanders in lieu of steam boilers [26]. Although this modification would not totally render the ammonia unit self-sufficient in terms of power consumption, it is claimed that the use of an expander would profit more rationally the thermo-mechanical exergy embodied in the reactor effluent. Since the exergy of the heat is transformed directly into work, the exergy losses due to the heat transfer driving forces and those related to the steam turbine condenser could be avoided. Furthermore, despite the power consumption and specific irreversibilities are still largely dependent on the expansion pressure, the specific work required per unit of mass of product is reported as 44-75% lower compared to the conventional boiler-based system [26]. Other authors studied a co-current gas-flowing/solids-fixed bed reactor (GFSFBR) [24], where the real time removal of the product from the reacting system shifts the equilibrium towards more ammonia production. Non-conventional approaches will be worthy to explore considering the current limited room for improvement in the reactive components. In fact, the highest exergy saving potentials are expected from the reevaluation of the high temperature gas-gas heat exchangers and the compression train [66], alongside with a reduction of the costly refrigeration. The energy-intensive nature of the current technical process is in fact mainly due to the large amount of exergy consumed in the makeup syngas compression, refrigeration and circulation systems (10.6 -14.4 MW).

Less optimistic studies [67] argue that, even if the ammonia unit losses were reduced in 60%, the total exergy losses in an 1,000 t/day integrated syngas and ammonia plant would decrease only about 6%, as long as the syngas production unit accounts for more than half of the exergy destruction. In the following, a comparison with other authors' work is briefly discussed.

Because of the non-linear dependence of the rate on the reaction driving force, Sauar et al. [53] applied the principle of equipartition of forces to demonstrate the suitability of the use of the isoforce operating lines for evaluating the trade-off between the augmentation of the ammonia throughput and the reduction of the entropy generation in the reactor. By promoting close to uniform driving forces along the reactor, this principle attempts to minimize the entropy production rate at a constant ammonia yield. The authors demonstrated that the optimum operation line (minimum entropy generation rate) lies between the line for the equilibrium and the state of maximum reaction rate. They also suggested that, by operating the reactor at 0.95 times the maximum reaction rate, the entropy production rate could be reduced by 31%. A smaller reaction rate means that nevertheless the reactor should be increased to maintain the ammonia yield.



Some authors [59] reported a significant effect on the power consumption of the fresh (makeup) gas compression with the variation of the temperature of cooling water. This effect is more critical in the amount of power required for the refrigeration compressor. Based on an ammonia plant operating at 140 bar, with a cooling water temperature of 30°C and ammonia product at -33°C, the exergy losses in the ammonia plant were reported for a typical 1,000 tons/day of ammonia plant. For the simulated case, the maximum exergy losses attained 26.7-29.0 MW in the ammonia loop, of which 67.2% are attributed to the ammonia synthesis and separation, and the remaining, to the compressor and turbine related losses.

Sorin and Brodyansky [68] presented a method for thermodynamic optimization that allows to target and reduce the *transformed exergy input* of the ammonia unit subsystems. These subsystems include the gas compression, the chemical transformation, the separation of reaction products and the recycling of non-reactive components. The analysis also involves the combustion of the purge gas. Since the synthesis loop operates at 270 bar, the authors analyzed the advantages of reducing the pressure and the suitability of increasing the ammonia separation by providing a lower temperature cooling utility. It has been found that, by decreasing the system pressure from 270 bar to 150 bar, the efficiency of the original system (74.3%) decreases only 2.3%.

Penkuhn et al. [66] compared the exergy efficiency of two ammonia loop configurations (1,600 t/day). The first configuration consists of a three stage adiabatic reactor (200 bar) with direct intercooling (quenching) and the second configuration consists of an intercooled reactor (140 bar) that uses Dowtherm A as coolant. The exergy efficiencies reported (90.78% for the cold-shot cooled and 96.39% for the indirect cooled case) approach those calculated by the *rational exergy* efficiency, whereas the exergy destroyed is significantly different in both designs (39.85 MW for the cold-shot cooled and 15.18MW for the indirect cooled case). This is a typical problem when calculating exergy efficiencies in large-volume chemicals production systems, such as ammonia plants, as discussed above. The authors concluded that the quenching process results in a higher exergy destruction and lower overall exergy efficiency. Moreover, the increase of the heat transfer coefficient reveals a certain improvement potential despite the almost unavoidable nature of the exergy destroyed in the reaction system. Also, the reactor design and pressure level have an important impact on the loop efficiency and the heat integration.

A comparative analysis between a conventional ammonia unit (refrigeration only) and two alternative ammonia loops with further recycled ammonia removal technologies has been reported by [69]. One alternative includes a water stripping process whereas the other uses pressure swing adsorption (PSA). The total exergy losses for a 1,000 metric ton per day plant range from 39.2 MW (PSA based) up to 41.0 MW (water scrubbing-based), with the conventional loop attaining 39.8 MW. According to the authors, the high solubility of ammonia in water renders the water stripping ammonia removal more energy intensive and less attractive, unless a fluid with less ammonia solubility is used. A more recent assessment [70] also uses water stripping for residual ammonia removal. The exergy destroyed in the ammonia loop (250 bar), calculated as 35.5 MW, represents almost one-third of the total exergy destroyed in the integrated syngas and ammonia production plant. Reduction of inerts content and reduced reactor outlet temperatures are envisaged as potential modifications that may drive losses down. Modified column designs could be helpful in reducing the amount of exergy destroyed in the residual ammonia removal system (9.64 MW).

Radgen and Lucas [71] performed a thermodynamic analysis of a fertilizer complex based on the pinch analysis and exergy analysis. In the authors' words, although the pinch analysis is more straightforward as a methodology to predict the backeffects of a change elsewhere in the loop, the exergy analysis allowed a more general view of the problem, not only limiting the improvement potentials to heat integration. On the other hand, exergy analysis demands a bigger effort as it requires explicitly the entropy function of the streams. For a 1,000 t/day ammonia loop, the total exergy destruction rate is reported about 30.9 MW of which 82.7% are only due to the syngas

compression, the steam production and the ammonia reactor. Other irreversibility sources are attributed to the ammonia removal and refrigeration, and purge gas purification systems. Further studies analyzed [12] the effect of the degree of conversion, the approach to equilibrium and the inert content (mol 7% CH<sub>4</sub>, 3% Ar) on the amount of irreversibilities of an ammonia loop operating at higher pressure (300 bar). The exergy destruction reported is as low as 18.06-18.95 MW for a single bed reactor-based loop, provided that no inerts are present in the reactor feed. A case study showed that the introduction of 10% of inerts on a 1,000 tons per day plant causes a marked increment (45.5%) on the exergy destruction rate, which is worsened if a poor degree of conversion and relatively high circulation ratio (5.7 kg gas/kg NH<sub>3</sub>) are considered.

All those results prove to be relevant in order to estimate the opportunities of improvement in the ammonia loop, when compared with the results obtained in this work. It is nevertheless important to point out that most of these works do not consider the effect of the variation of other loop parameters such as bed intercooling, feed composition and loop pressure, and some of them were performed on the basis of energy data and assumed Carnot factors for specific temperature levels.

Figure 6 show the overall exergy efficiency of the unit as defined by Eqs. (9-12). It is observed that the *rational* and at some extent, the *relative* exergy efficiency, are almost insensitive to the variation of the process parameters. On the other hand, both *transit* and *recovery* definitions reflect better the loop performance since they only take into account the effect of the loop parameters on the performance of the chemical unit.

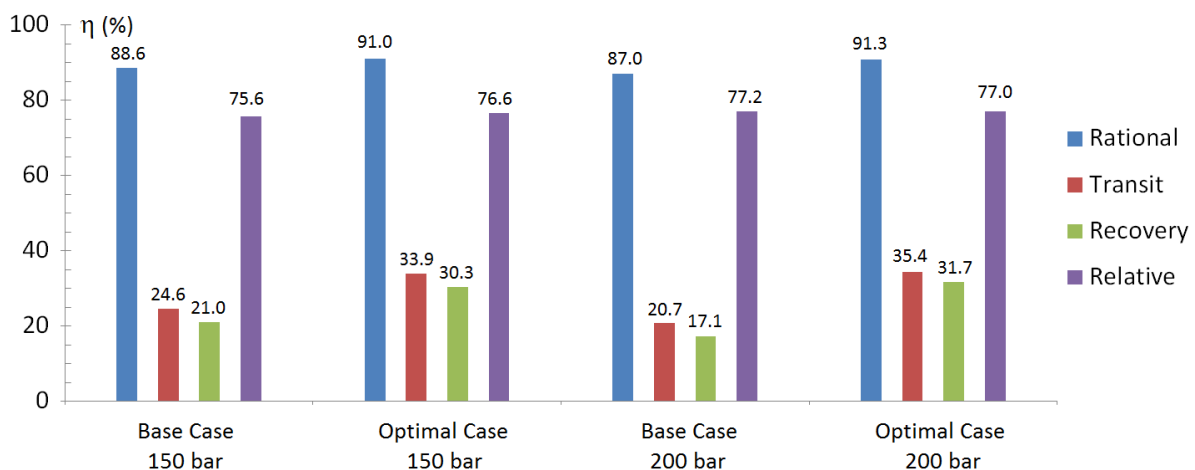


Fig. 6. Plant-wide exergy efficiencies: base-case and optimal case.

Transit efficiency definition is slightly higher than the recovery efficiency since, as mentioned in section 3.1.2, it assumes that all the non-reacted nitrogen and hydrogen is recycled back to the ammonia converter and only liquid pure ammonia, methane and argon exit the loop. In other words, neither offgas production nor low pressure hydrogen-rich stream are considered. Besides, the term  $B_{BFW}^{PH}$  in Eq. (10) is considered as an input exergy quantity, and not as transit exergy in the waste heat boiler. The numerator in Eq. (10) has been originally proposed in terms of the electricity generated in an additional energy conversion process, e.g. an associated Rankine cycle (100 bar) [12]. However, in this work, the boundaries of the system studied are restricted to the steam generation process. The reason is that the recovery of the reaction enthalpy in the form of steam is actually linked to a more complicated combined steam and power production system in the integrated syngas and ammonia production plant, as described in Ref. [1]. Furthermore, fixed the available header pressure levels in the steam network system, there is not necessarily a direct relation between the power cycle performance and the ammonia loop parameters, since the steam system should be able to compensate the heat recovery network deficit. Accordingly, the loop performance and the available steam generation potential are suitably estimated by the *recovery*

efficiency definition, which attempts to determine the opportunity to recover all the dissipated heat to the extent of the process limitation (i.e. an exothermic, equilibrium and rate limited, high temperature reactive system), in the form of a valuable ammonia unit subproduct, namely, high pressure steam. In fact, increased system pressure and temperature also increases the exergy available in the process gas and the high pressure steam production is improved.

On the other hand, the *relative* efficiency has been defined by using the minimum theoretical exergy consumption required to produce ammonia from the elements in the environment. As such, the relative efficiency accounts for the maximum potential of energy savings, including the upstream production processes of nitrogen and hydrogen. But, notwithstanding its broader scope and improved sensitivity compared to the abnormally higher *rational* efficiency, this indicator still presents part of the shortcomings posed by the efficiency definitions of bulk chemicals production processes with large flow rates. In an attempt to differentiate between the transiting exergy and the consumed exergy, Sorin and Paris [72] defined the ‘transiting exergy in the utilizable stream’. They calculated it as the part of the exergy entering a unit operation and traversing it without undergoing any transformation, leaving the system with the ‘utilizable stream’. However, due to the fact that the main loop effluent, namely the ammonia produced, has been actually transformed, apart from the small amount of feedstock in the purge and the traces dissolved in ammonia, no other stream cannot be considered as *transit exergy*.

Finally, Figs.(7-8) detail the exergy efficiencies of representative components of the ammonia loop operating under the base and best case setups for each pressure studied.

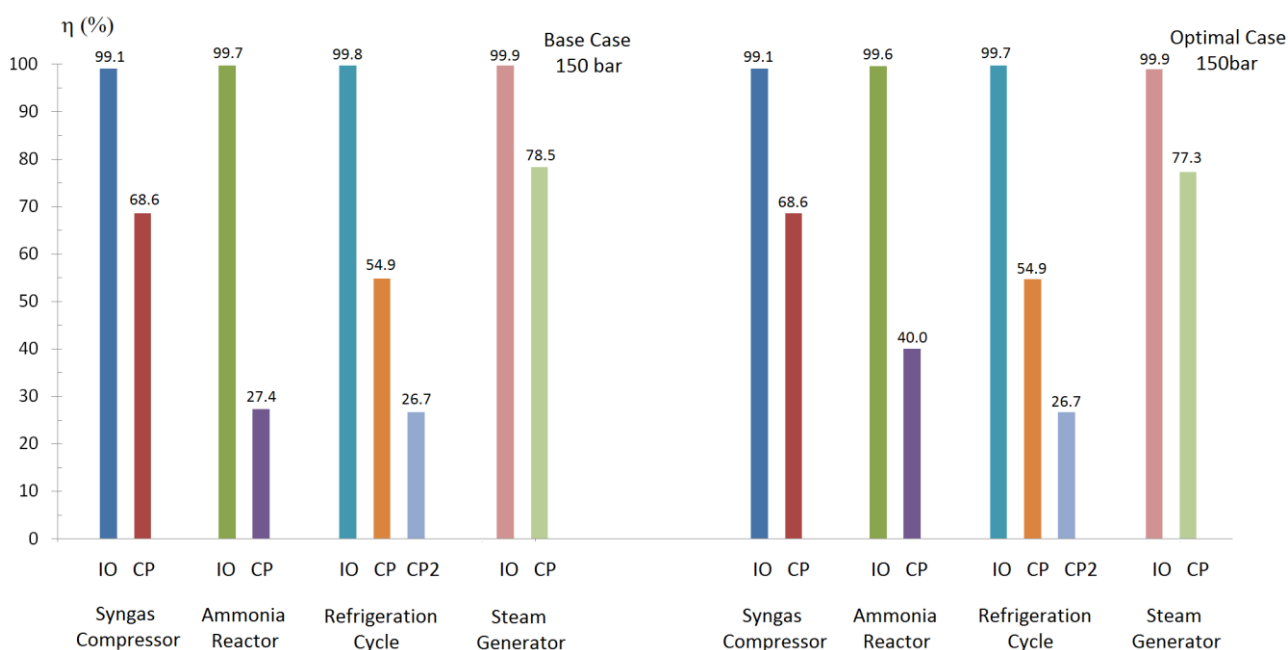


Fig. 7. Exergy efficiencies for representative components of the ammonia loop (150 bar).

It is interesting to remark the difference in the results obtained from the three exergy efficiency definitions for the refrigeration cycle. Since the consumed produced efficiency CP2 includes the exergy destroyed in the control volume of the evaporator, the exergy efficiency is appreciable lower than in the case in which it is only considered the exergy of the heat transferred at -30°C. Regarding to the syngas compressor efficiency, the consumed-produced exergy efficiency is quite similar for any operating pressure and base-case/optimal condition. It is not the same for the ammonia reactor efficiency for the base-case conditions, which is at least 40% lower compared to the optimal cases. Moreover, it is not surprising that the consumed-produced exergy efficiencies in the refrigeration cycle are similar in all the cases, considering that the isentropic efficiency of the refrigeration

compressors is assumed equal, and the compression ratios were selected to reduce the refrigeration power consumption.

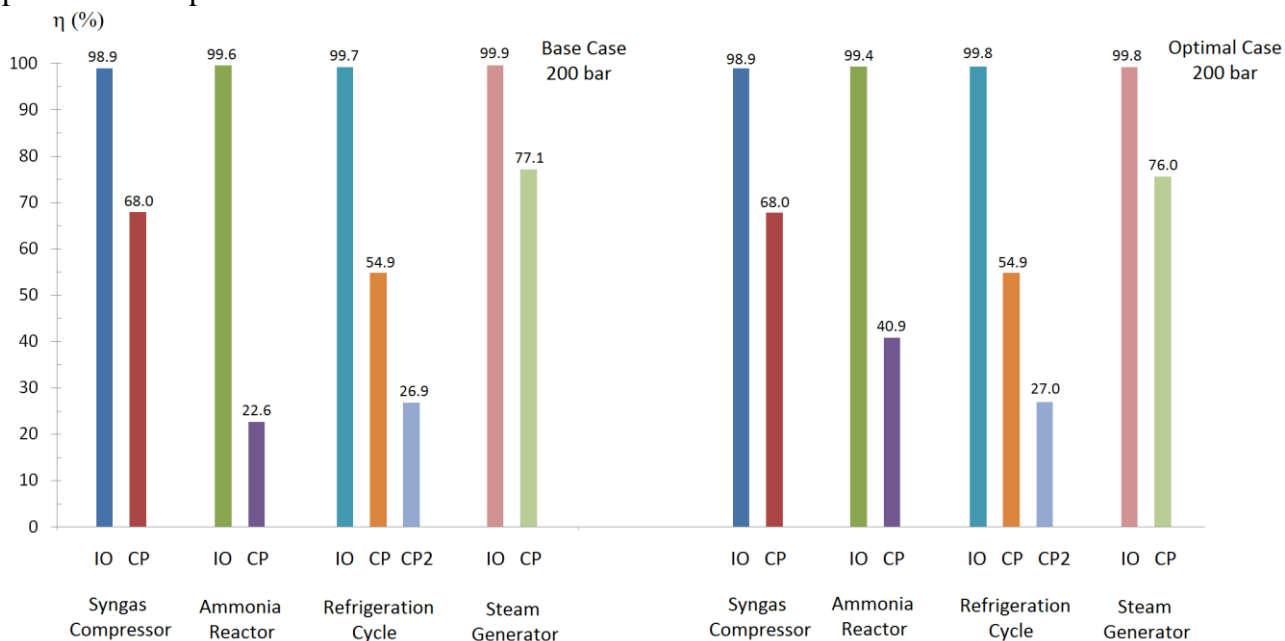


Fig. 8. Exergy efficiencies for representative components of the ammonia loop (200 bar).

#### 4.4. Exergy destruction: case studies.

Since the ammonia unit performance is fundamentally determined by the reactor parameters, followed by the purge and recycle rates and the refrigeration duty, in the case that one of them abruptly changes, the other parameters will change until the steady state is again achieved [59]. Thus, the chemistry and thermodynamics of the process define a window of possible operating conditions at which the ammonia synthesis is feasible, and out of which no convergence of mass, energy and exergy balances could be obtained [59]. As the number of independent variables increases, the computational effort for solving the optimization problem increases substantially, particularly for reactor-separator-recycle systems, because of their intricate non-linear characteristics [73]. Therefore, in order to determine a feasible dominion for the optimization problem, the effect of the most important parameters on the loop performance has been evaluated through a series of case studies. The most interesting of such case studies is the determination of the exergy destruction rate as a function of the catalytic bed inlet temperatures  $T_1$  and  $T_3$  for different fresh syngas  $H_2/N_2$  ratios (Figs. 9-10). These plots are used to explore the boundaries of the feasible region where the studied parameters satisfy the imposed restrictions, and they could be, therefore, understood as feasible maps of the chemical process. It is important to point out that, differently from the SP150 case for which the maps exhibit a similar behavior, the case studies shown for SP200 they are highly dependent on the  $H_2/N_2$  ratio. A marked increase of the exergy destruction is observed for the cases in which the fresh syngas  $H_2/N_2$  ratio is about 2.832 ( $H_2/N_2 \sim 1$  in the reactor feed stream). When dealing with exothermic autothermal reactors that present instability points (near *blow off* operation states), the convergence of the process simulation is hindered, which renders the process synthesis and flowsheet optimization a challenging task.

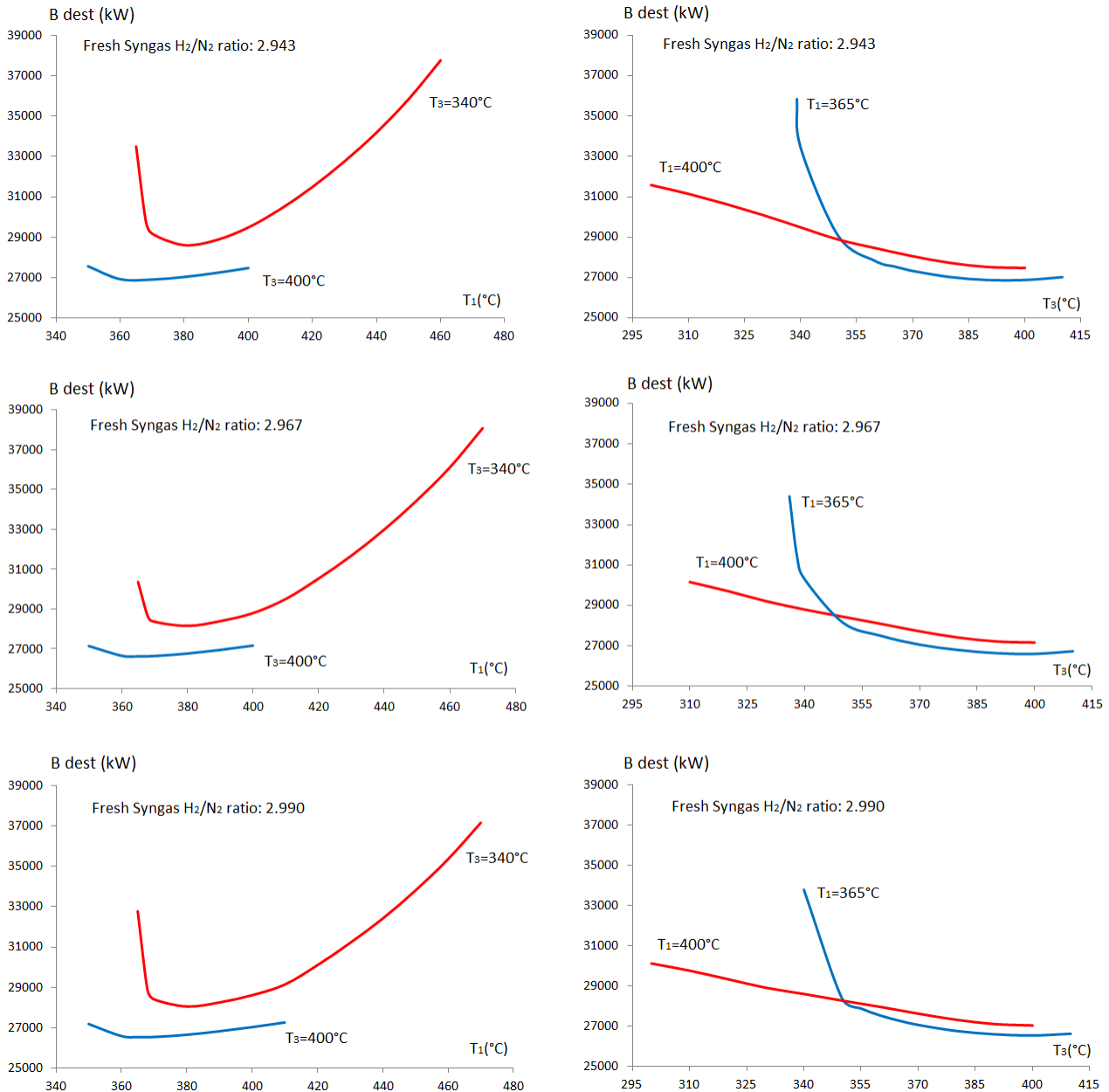


Fig. 9. Exergy destruction in the ammonia loop as a function of the catalytic bed inlet temperatures  $T_1$  and  $T_3$  (Loop pressure: 150 bar).

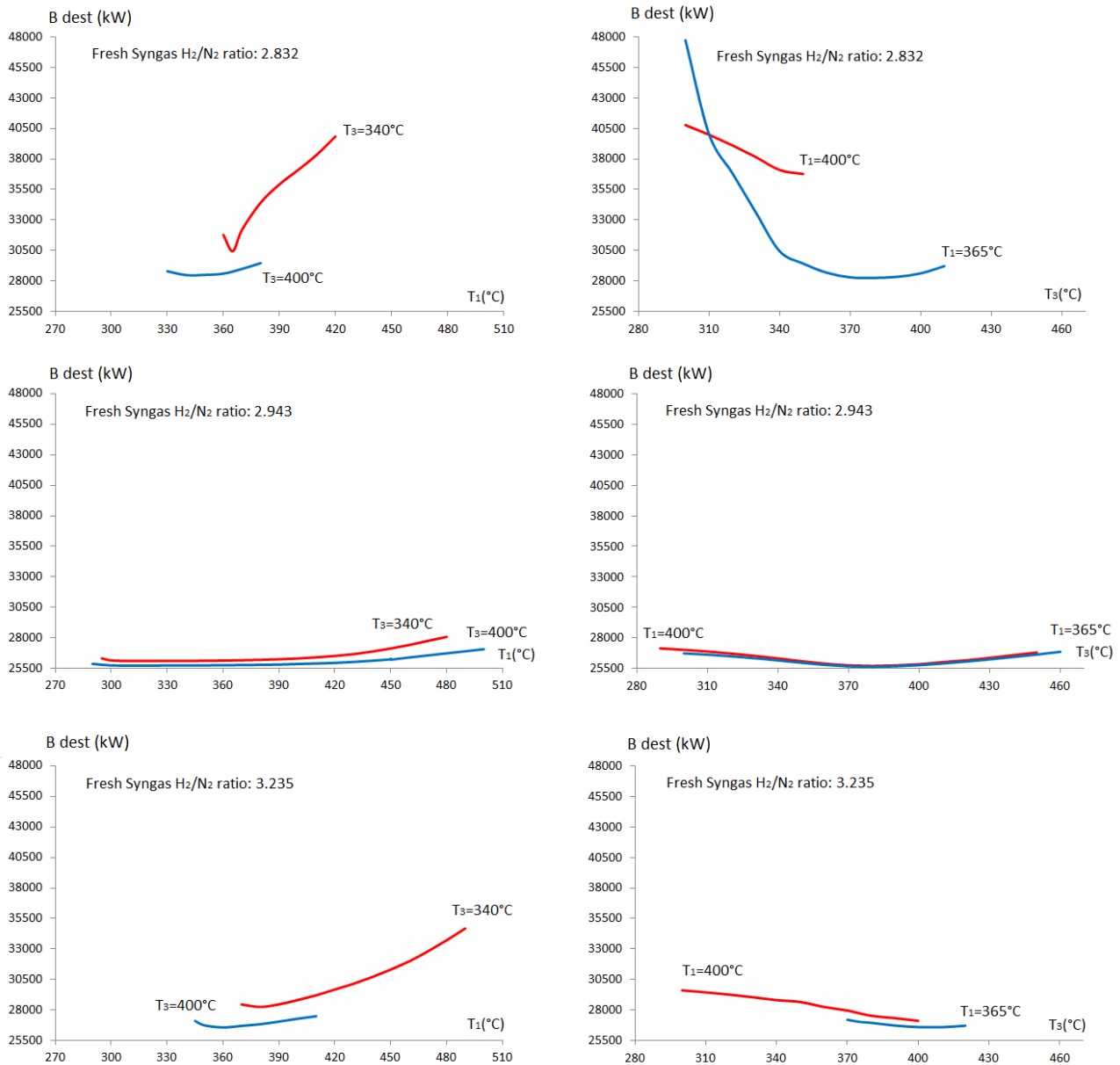


Fig. 10. Exergy destruction in the ammonia loop as a function of the catalytic bed inlet temperatures  $T_1$  and  $T_3$  (Loop pressure: 200 bar)

## 5. Conclusions

The interrelation between the inlet temperature, reaction kinetics and catalytic beds arrangement and its effects in the performance of the ammonia condensation and heat recovery network renders the ammonia synthesis an interesting application for evaluating the limitations on the parametric optimization of exothermic (equilibrium-limited) processes at high temperatures and pressures that present recycle/purge streams. Two different suitable approaches are proposed in order to calculate the exergy efficiency of large volume chemicals production, such as ammonia. Those systems lack of a convenient way of calculating the exergy efficiency due to the large ratio of the exergy of mass streams to the exergy flows rates (power and heat). Some exergy definitions struggle with the fact that the chemical exergy is internally converted into other forms of exergy and exported in the form of steam, flue gas and ammonia product, which renders the application of the transit exergy concept inapplicable. A series of case studies that allows determining the feasible dominion of where the constraints imposed by the first and second law of thermodynamics are satisfied while the problem of the exergy destruction minimization is also presented. Even at optimal operating conditions, the

ammonia synthesis reactor, the syngas compression, the ammonia refrigeration and the waste heat recovery system are together responsible for about 26 MW of exergy destruction. Better catalysts (higher activities and higher reaction rates at lower pressures), and enhanced converter designs (dual pressure systems, multiple beds) along with improved waste heat recovery and more efficient refrigeration/condensation systems must be pursued if a higher yield and lower exergy destruction is aimed. Moreover, it has been found that, despite increasing the driving forces may imply higher exergy destruction rates according to the Counteraction Principle, by solely increasing the reacting driving forces in the ammonia converter, the whole system irreversibilities are not necessarily increased, since the global effect of the finite driving forces in that equipment may be compensated by the enhancement of the performance of the integrated chemical unit. Thus, the minimization of the large amount of exergy consumed in the industrial ammonia units is rather a trade-off between lower exergy destruction rates and higher ammonia yields. In any case, the minimization of the exergy destruction is not a priori an economic criterion, since this task is often achieved at the expense of large capital investments. It is therefore necessary to discuss not only the relationship between the overall exergy destruction, but also its distribution through the process, and the economy thereof [74].

## Acknowledgments

The first author would like to acknowledge the National Agency of Petroleum, Gas and Biofuels – ANP and its Human Resources Program (PRH/ANP Grant 48610.008928.99), and the Administrative Department of Science, Technology and Innovation – COLCIENCIAS for supporting the first stage of this work. He also would like to knowledge the Swiss Government Excellence Scholarship program (2016.0876) and the Ecole Polytechnique Federal de Lausanne for supporting the second stage of this study. Second author would like to thank National Research Council for Scientific and Technological Development, CNPq (grant 306033/2012-7)

## Nomenclature

### Latin Symbols

$n$	Nitrogen molar flow	$\text{kmol h}^{-1}$
$a$	Activity coefficient	--
$B$	Exergy rate	$\text{kW}$
$\text{BFW}$	Boiler feedwater	--
$b^{\text{CH}}$	Standard chemical exergy	$\text{kJ kmol}^{-1}$
$Q$	Heat transfer rate	$\text{kW}$
$W$	Power	$\text{kW}$
$G$	Superficial mass velocity of reactants	$\text{kg s}^{-1} \text{m}^{-2}$
$C_p$	Specific heat capacity	$\text{kJ kmol}^{-1} \text{K}^{-1}$
$H$	Enthalpy	$\text{kW}, \text{kJ}$
$S$	Entropy	$\text{kW}, \text{kJ}$
$E_a$	Activation energy	$\text{kJ kmol}^{-1}$
$r$	Rate of nitrogen reaction	$\text{kmol m}^{-3} \text{cat}^{-1} \text{h}^{-1}$
$V$	Reactor volume	$\text{m}^3$
$K_p^2$	Equilibrium constant	--
$k_f$	Forward reaction constant	--
$k_b$	Backward reaction constant	--
$f$	Mixture component fugacity	$\text{atm}$
$f^\circ$	Pure component fugacity	$\text{atm}$
$x_i$	Species mol fraction in liquid phase	--

$y_i$	Species mol fraction in vapor phase	--
$P$	Total reactor pressure	bar
$z$	Reactor length	m
$D_p$	Catalyst effective diameter	m
$S_{gen}$	Entropy generation rate	$\text{kJ K}^{-1} \text{h}^{-1}$
$T$	Temperature	$^{\circ}\text{C}, \text{K}$
$T_R$	Reference temperature	$^{\circ}\text{C}, \text{K}$
$T_o$	Ambient temperature	$^{\circ}\text{C}, \text{K}$
$\Delta H_R^{\circ}$	Reaction enthalpy	$\text{kJ kmol}^{-1}$
$\Delta G$	Gibbs energy of reaction difference	$\text{kJ kmol}^{-1}$
$R_u$	Ideal gas constant	$\text{kJ kmol}^{-1} \text{K}^{-1}$

### Greek Symbols

$\xi$	Reactor conversion	--
$\mu$	Dynamic viscosity	$\text{kg s}^{-1} \text{m}^{-1}$
$\rho$	Gas density	$\text{kg m}^{-3}$
$\gamma_i$	Species activity coefficient	--
$\alpha$	Temkin-Phyzev's exponent	--
$\phi$	Void fraction	--
$\Theta_i$	Molar flow ratio $i$ to nitrogen at the reactor inlet	--
$\phi'_i$	Fugacity coefficient of species $i$	--
$\eta$	Efficiency	--

### Superscript and subscript

PH	Physical exergy
CH	Chemical exergy
CP	Consumed-produced efficiency
o	Ambient conditions
R	Reference conditions
M	Mass-associated exergy
Q	Heat-associated exergy
Dest	Destroyed
H	High level temperature
L	Low level temperature

### References

- Flórez-Orrego, D., Oliveira Junior, S., *On the efficiency, exergy costs and CO2 emission cost allocation for an integrated syngas and ammonia production plant*. Energy, 2016. 117, Part 2: p. 341-360.
- PETROBRAS. Facts and data: Understand why we invest in fertilizers [In Portuguese] (2014), Accessed: 14.12.2016; Available from: <http://www.petrobras.com.br/fatos-e-dados/entenda-por-que-investimos-em-fertilizantes.htm>.
- FAO. Current world fertilizer trends and outlook to 2015 (2011). Accessed 15.10.16; Available from: <ftp://ftp.fao.org/ag/agp/docs/cwfto15.pdf>
- Ribeiro, P.H., Contribution to the brazilian databank for supporting the life cycle assessment: nitrogen fertilizers [In portuguese], in Polytechnic School, Department of Chemical Engineering.2009, University of Sao Paulo: Sao Paulo.
- Hernandez, M., Torero, M., Fertilizer Market Situation: Market Structure, Consumption and Trade Patterns, and Pricing Behavior. IFPRI Discussion Paper 01058. International Food Policy Research Institute. January 2011.
- Dias, V., Fernandes, E., Fertilizers: A global vision [In portuguese]. BNDES Setorial, RJ, set.2006, (24): p. 97-138.
- CIESP. Fertilizers: Petrobras expands its actuation, may 12, 2014 [In Portuguese] (2014). Accessed 14.05.14; Available from: <http://www.ciesp.com.br/cubatao/noticias/fertilizantes-petrobras-amplia-atuacao>.



8. Portal Brasil, Dilma: "To produce fertilizer is strategic to Brazil", *Infraestrutura, Nitrogenados*, [In Portuguese] 03/05/2014. Portal Brasil, 2014.
9. Papoulias, S., Grossmann, I., *A structural optimization approach in process synthesis—III: Total processing systems*. Computers & Chemical Engineering, 1983. **7**(6): p. 723-734.
10. Worrell, E., Blok, K., *Energy savings in the nitrogen fertilizer industry in the Netherlands*. Energy, 1994. **19**(2): p. 195-209.
11. Leites, I.L., Sama, D. A., Lior, N., *The theory and practice of energy saving in the chemical industry: some methods for reducing thermodynamic irreversibility in chemical technology processes*. Energy, 2003. **28**(1): p. 55-97.
12. Kirova-Yordanova, Z., *Exergy analysis of industrial ammonia synthesis*. Energy, 2004. **29**(12–15): p. 2373-2384.
13. Panjeshahi, M.H., Ghasemian Langeroudi, E., Tahouni, N., *Retrofit of ammonia plant for improving energy efficiency*. Energy, 2008. **33**(1): p. 46-64.
14. Tock, L., Maréchal, F., Perrenoud, M., *Thermo-environomic evaluation of the ammonia production*. The Canadian Journal of Chemical Engineering, 2015. **93**(2): p. 356-362.
15. BCInsight, *Ultra-mega plants - An assessment*. Fertilizers International 444, 2011(September-October): p. 38-43.
16. Appl, M., *Ullmann's encyclopedia of industrial chemistry, Vol.11. Chapter 2.*, Wiley-VCH, Editor. 2012, Wiley-VCH Verlag GmbH & Co., Weinheim.
17. Kirova-Yordanova, Z., *Thermodynamic Evaluation of Energy Integration and Cogeneration in Ammonium Nitrate Production Complexes*. International Journal of Thermodynamics, 2013. **16**(4): p. 163-171.
18. Rafiqul, I.W., C., Lehmann, B., Voss, A., *Energy efficiency improvements in ammonia production—perspectives and uncertainties*. Energy, 2005. **30**(13): p. 2487-2504.
19. Dopfer, J.G., *European Roadmap for Process Intensification*. 2007, Ministry of Economic Affairs: Delft, The Netherlands. p. 53.
20. Canadian Fertilizer Institute, *Benchmarking energy efficiency and carbon dioxide emissions*. 2007, Canadian Industry Program for Energy Conservation.
21. Liu, H., *Ammonia Synthesis Catalysts: Innovation and Practice*. 2013, Beijing: Chemical Industry Press, ISBN 978-981-4355-77-3.
22. Leveson, P.D., *Thermally Coupled Monolith Reactor*, US 20070009426 A1. 2007, ZeroPoint Clean Technologies Inc.: United States. p. 12.
23. Hinderink, A., Kerckhof, F., Lie, A., De Swaan Arons, J., Van Der Kooi, H., *Exergy analysis with a flowsheeting simulator—II. Application; synthesis gas production from natural gas*. Chemical Engineering Science, 1996. **51**(20): p. 4701-4715.
24. Nikačević, N., Jovanović, M., Petkovska, M., *Enhanced ammonia synthesis in multifunctional reactor with in situ adsorption*. Chemical Engineering Research and Design, 2011. **89**(4): p. 398-404.
25. Sahafzadeh, M., Ataei, A., Tahouni, N., Panjeshahi, M., *Integration of a gas turbine with an ammonia process for improving energy efficiency*. Applied Thermal Engineering, 2013. **58**(1–2): p. 594-604.
26. Greeff, I.L., Visser, J. A., Ptasinski, K. J., Janssen, F. J. J. G., *Integration of a turbine expander with an exothermic reactor loop—Flow sheet development and application to ammonia production*. Energy, 2003. **28**(14): p. 1495-1509.
27. Mudahar, M., Hignett, T., *Energy efficiency in nitrogen fertilizer production*. Energy Agric, 1985. **4**: p. 159-177.
28. Tamaru, K., *The History of the Development of Ammonia Synthesis*, in *Catalytic Ammonia Synthesis*, J.R. Jennings, Editor. 1991, Springer US. p. 1-18.
29. Maxwell, G., *Synthetic Nitrogen Products: A Practical Guide to the Products and Processes* 2004, New York: Springer US.
30. Ostuni, R., Filippi, E., Skinner, G.F., *Hydrogen and Nitrogen Recovery from Ammonia Purge Gas*. US 20130039835 A1. 2013, Ammonia Casale SA.
31. Florez-Orrego, D., Oliveira Jr., S. *Exergy Assessment of Single and Dual Pressure Ammonia Production Plants in International Conference on Contemporary Problems of Thermal Engineering - CPOTE 2016*. 2016. Gliwice, Poland.
32. Péneloux, A., Rauzy, E., Fréze, R., *A consistent correction for Redlich-Kwong-Soave volumes*. Fluid Phase Equilibria, 1982. **8**(1): p. 7-23.
33. ASPENTECH, *Aspen Physical Property System - Physical Property Methods V7.3 - User Guide*. 2011.
34. ASPENTECH, *Aspen Plus - Aspen Plus Ammonia Model*. 2008.
35. Abdollahi-Demneh, F., Moosavian, M., Omidkhan, M., Bahmanyar, H., *Calculating exergy in flowsheeting simulators: A HYSYS implementation*. Energy, 2011. **36**(8): p. 5320-5327.
36. Turton, R.B., R. Whiting, W., Shaeiwitz, J., *Analysis, Synthesis and Design of Chemical Processes*. 3rd ed. 2009, New York: Prentice Hall.
37. Dyson, D.C., Simon, J. M., *Kinetic Expression with Diffusion Correction for Ammonia Synthesis on Industrial Catalyst*. Industrial & Engineering Chemistry Fundamentals, 1968. **7**(4): p. 605-610.
38. Gillespie, L., Beattie, J. A., *The Thermodynamic Treatment of Chemical Equilibria in Systems Composed of Real Gases. I. An Approximate Equation for the Mass Action Function Applied to the Existing Data on the Haber Equilibrium*. Physical Review, 1930. **36**(4): p. 743-753.
39. Singh, C.P., Saraf, D. N., *Simulation of Ammonia Synthesis Reactors*. Industrial & Engineering Chemistry Process Design and Development, 1979. **18**(3): p. 364-370.

40. Fogler, S.H., *Elements of Chemical Reaction Engineering*. 4th Edition ed. 1986: Prentice-Hall.
41. Imperial Chemical Industries, *Catalyst handbook: With special reference to unit processes in ammonia and hydrogen manufacture*. 1970: Wolfe Publishers.
42. Sandler, S., Orbey, H., *Modeling Vapor-Liquid Equilibria: Cubic Equations of State and Their Mixing Rules*, Cambridge University Press. 1998: Cambridge Series on Chemical Engineering.
43. Szargut, J., Morris, D., Steward, F., *Exergy analysis of thermal, chemical, and metallurgical processes*. 1988, New York: Hemisphere Publishing Corporation.
44. Sorin, M., Lambert, J., Paris, J., *Exergy Flows Analysis in Chemical Reactors*. Chemical Engineering Research and Design, 1998. **76**(3): p. 389-395.
45. Tsatsaronis, G., *Thermoeconomic analysis and optimization of energy systems*. Progress in Energy and Combustion Science, 1993. **19**(3): p. 227-257.
46. Szargut, J., *Exergy in thermal systems analysis*, in *Thermodynamic optimization of complex energy systems*, NATO Science Series 69, A. Bejan, Mamut, E., Editors. 1999, Springer.
47. Brodyansky, V.M., Sorin, M.V. and Le Goff, P., *The Efficiency of Industrial Processes: Exergy Analysis and Optimization*. 1994, Amsterdam: Elsevier.
48. Denbigh, K.G., *The second-law efficiency of chemical processes*. Chemical Engineering Science, 1956. **6**(1): p. 1-9.
49. Appl, M., *Ammonia: Principles and Industrial Practice*. 1999, New York: Wiley-VCH Verlag.
50. Jacobsen, C., Dahl, S., Boisen, A., Clausen, B., Topsøe, H., Logadottir, A., Nørskov, J. K., *Optimal Catalyst Curves: Connecting Density Functional Theory Calculations with Industrial Reactor Design and Catalyst Selection*. Journal of Catalysis, 2002. **205**(2): p. 382-387.
51. Chorkendorff, I., Niemantsverdriet, J. W., *Concepts of Modern Catalysis and Kinetics*. 2nd ed. 2007: Wiley-VCH Verlag GmbH & Co, ISBN: 978-3-527-31672-4.
52. Kandiyoti, R., *Fundamentals of Reaction Engineering*. 2009: Ventus Publishing APS.
53. Saunar, E., Nummedal, L., Kjelstrup, S., *The principle of equipartition of forces in chemical reactor design: The ammonia synthesis*. Computers & Chemical Engineering, 1999. **23**: p. S499-S502.
54. UNIDO, Fertilizer Manual: UN Industrial Development Organization. 3rd ed, 1998, Dordrecht, Netherlands: Kluwer Academic Publishers. 616pp.
55. Froment, G., Bishoff, K. Wilde, J., *Chemical Reactor Analysis and Design*. 3ed. 2010, New York: John Wiley and Sons.
56. Seider, W., Seader, J., Lewin, D., *Product Process and Design Principles: Synthesis, Analysis and Evaluations*. 2nd ed. 2004: John Wiley and Sons. 1122.
57. van der Ham, L.V., J. Gross, and S. Kjelstrup, *Two performance indicators for the characterization of the entropy production in a process unit*. Energy, 2011. **36**(6): p. 3727-3732.
58. Knopf, C., *Modeling, Analysis and Optimization of Process and Energy Systems*, 1st ed., 2011: Wiley, ISBN: 978-0-470-62421-0.
59. Nielsen, A., *Ammonia: Catalysis and Manufacture*. ISBN 9783540583356. 1995: Springer.
60. Hocking, M.B., Ch. 11 - *Ammonia, nitric acid, and their derivatives*, in *Handbook of Chemical Technology and Pollution Control*, 1998, Academic Press: San Diego. p. 311-354.
61. Grossmann, I., *Mixed-integer programming approach for the synthesis of integrated process flowsheets*. Computers & Chemical Engineering, 1985. **9**(5): p. 463-482.
62. Rangaiah, P., *Stochastic Global Optimization: Techniques and Applications in Chemical Engineering*. 2010: World Scientific.
63. Kjelstrup, S., de Swaan Aaron, J., *Denbigh revisited: Reducing lost work in chemical processes*. Chemical Engineering Science, 1995. **50**(10): p. 1551-1560.
64. Flórez-Orrego, D., Oliveira Jr, S. *On the Allocation of the Exergy Costs and CO<sub>2</sub> Emission Cost for an Integrated Syngas and Ammonia Production Plant*. in *28th International Conference on Efficiency, Cost, Optimization, Simulation and Environmental Impact of Energy Systems, ECOS 2015*. 2015. Pau, France.
65. Silva, J.A.M., Flórez-Orrego, D., Oliveira Jr, S., *An exergy based approach to determine production cost and CO<sub>2</sub> allocation for petroleum derived fuels*. Energy, 2014. **67**(0): p. 490-495.
66. Penkuhn, M., Tsatsaronis, G., *Comparison of different ammonia synthesis loop configurations with the aid of advanced exergy analysis*, in *29th International Conference on Efficiency, Cost, Optimization, Simulation and Environmental Impact of Energy Systems, ECOS 2016*. 2016: Portoroz, Slovenia.
67. Maansson, B., Andresen, B., *Optimal temperature profile for an ammonia reactor*. Industrial & Engineering Chemistry Process Design and Development, 1986. **25**(1): p. 59-65.
68. Sorin, M.V., Brodyansky, V. M., *A method for thermodynamic optimization—I. Theory and application to an ammonia-synthesis plant*. Energy, 1992. **17**(11): p. 1019-1031.
69. DOE, *Evaluation of Alternative Technologies for Ethylene, Caustic-Chlorine, Ethylene Oxide, Ammonia, and Terephthalic Acid I*. JVP International, 2007, Departamento of Energy, Industrial Technologies Program: New York. p. 135.
70. Ghannadzadeh, A., Sadeqzadeh, M., *Diagnosis of an alternative ammonia process technology to reduce exergy losses*. Energy Conversion and Management, 2016. **109**: p. 63-70.

71. Radgen, P., Lucas, K., *Energy system analysis is fertilizer complex – pinch analysis vs. Exergy analysis*. Chemical Engineering & Technology, 1996. **19**(2): p. 192-195.
72. Sorin, M., Paris, J., *Integrated exergy load distribution method and pinch analysis*. Computers & Chemical Engineering, 1999. **23**(4-5): p. 497-507.
73. Biegler, L.T., Grossmann, I.E., Westerberg, A.W., *Systematic methods for chemical process design*. 1997: Prentice Hall. 700pp.
74. Tondeur, D., Kvaalen, E., *Equipartition of entropy production. An optimality criterion for transfer and separation processes*. Industrial & Engineering Chemistry Research, 1987. **26**(1): p. 50-56.